Fakultät für Medizin

Neurologische Klinik und Poliklinik

The Brain in Pain:
Altered Resting-state EEG in Chronic Pain

Son Ta Dinh

Vollständiger Abdruck der von der Fakultät für Medizin der Technischen Universität München zur Erlangung des akademischen Grades eines

Doctor of Philosophy (Ph.D.)

genehmigten Dissertation.

Vorsitzender: Prof. Dr. Claus Zimmer

Betreuer: Prof. Dr. Markus Ploner

Prüfer der Dissertation:

1. Prof. Dr. Paul Sauseng

2. Priv.-Doz. Dr. Valentin Riedl

Die Dissertation wurde am 01.08.2019 bei der Fakultät für Medizin der Technischen Universität München eingereicht und durch die Fakultät für Medizin am 22.10.2019 angenommen.

Contents

List of Tables

List of Figures

Abstract

Chronic pain is a common and severely disabling disease whose treatment is often unsatisfactory and whose neural mechanisms are incompletely understood. Here, we aimed to harness the potential of electroencephalography (EEG) to determine abnormalities of brain function during the resting-state in chronic pain. We therefore performed state-of-the-art analyses of oscillatory brain activity, brain connectivity and brain networks in 101 chronic pain patients and a healthy control group of 84 pain-free participants. We observed significantly increased connectivity at theta (4 – 8 Hz) and gamma (> 60 Hz) frequencies in frontal brain areas and global network reorganization at gamma frequencies in chronic pain patients. A machine learning algorithm could differentiate between patients and healthy controls with an above-chance accuracy of 57 percent, mostly based on frontal connectivity. These results implicate increased theta and gamma synchrony in frontal brain areas in the pathophysiology of chronic pain. Beyond, the findings might represent a step further towards a low-cost, broadly available and potentially mobile brain-based marker and a novel treatment target of chronic pain.

Zusammenfassung

Chronischer Schmerz ist eine weitverbreitete und sehr belastende Krankheit, deren Behandlung oft unbefriedigend verläuft und deren exakte neuronale Mechanismen noch unklar sind. Mit dem Ziel das Potential von EEG auszuschöpfen, wurde die Hirnaktivität von Patienten mit chronischen Schmerzen untersucht und mit der Hirnaktivität von gesunden Probanden verglichen. Dazu wurden modernste Analysen der oszillatorischen Hirnaktivität, -konnektivität und der Netzwerkarchitektur des Gehirns bei 101 Patienten mit chronischen Schmerzen und einer Kontrollgruppe mit 84 gesunden und schmerzfreien Probanden durchgeführt. In der Gruppe der Patienten zeigte sich eine signifikant erhöhte Konnektivität in den Theta- (4 – 8 Hz) und Gamma-Frequenzen (> 60 Hz) in frontalen Hirnarealen und eine globale Netzwerk-Umstrukturierung in Gamma-Frequenzen. Mit Hilfe von maschinellem Lernen konnte zwischen Patienten und gesunden Kontrollprobanden mit einer Genauigkeit von 57 Prozent unterschieden werden, vornehmlich auf Basis frontaler Konnektivität. Diese Ergebnisse deuten darauf hin, dass erhöhte Theta- und Gamma-Synchronität in frontalen Hirnarealen eine bedeutende Rolle in der Pathophysiologie von chronischem Schmerz spielen. Diese Befunde sind ein weiterer Schritt auf dem Weg in Richtung eines kosteneffizienten, allgemein verfügbaren und potenziell mobilen Hirn-basierten Biomarkers. Darüber hinaus könnten die Befunde dazu dienen, neue Ansatzpunkte für chronische Schmerztherapien zu generieren.

Acronyms

AEC orthogonalized amplitude envelope correlation. 28, 34, 38, 39, 40, 41, 42, 47, 48, 49, 55

dwPLI debiased weighted phase lag index. 28, 30, 34, 38, 42, 43, 44, 47, 48, 49, 51, 55

EEG electroencephalography. 1, 9, 12, 13, 14, 15, 17, 19, 20, 21, 23, 26, 28, 29, 31, 34, 35, 38, 50, 53, 54, 55, 56, 57, 58

PLV phase locking value. 28, 30, 34, 38, 39, 40, 41, 42, 43, 47, 48, 49, 51, 55

SVM support vector machine. 21, 31, 32, 33, 34, 50, 51, 55, 57, 58

1 Introduction

1.1 Definition and Relevance of Pain

According to the International Association for the Study of Pain (IASP), "Pain is an unpleasant sensory and emotional experience associated with actual or potential tissue damage, or described in terms of such damage" (Merskey and Bogduk, 1994). This definition implies the contribution of multiple aspects to the pain experience, both a sensory aspect, mediated by a specialized transmission system between the periphery and the spinal cord, and an emotional and cognitive aspect, mediated by higher-level cognitive processes in the brain.

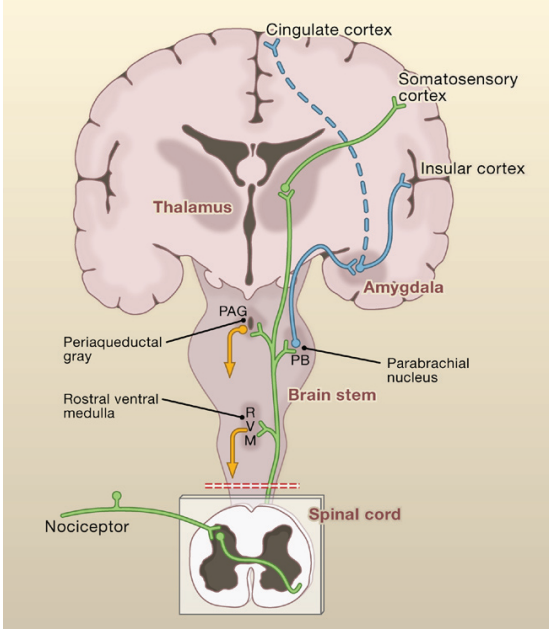

Figure 1: Anatomy of the nociceptive pathway.

A schematic of the major nociceptive pathway from the periphery's nociceptors through the spinal cord to the brain and back. From the dorsal horn of the spinal cord, a subset of neurons project to the somatosensory cortex via the thalamus, while other populations of neurons project to the cingulate and insular cortices via connections in the brain stem and amygdala. This ascending information is also modulated by neurons of the rostral ventral medulla and the periaqueductal gray which are associated with the descending feedback systems that regulate the output from the spinal cord. Adapted from Basbaum et al. (2009) with permission (originally published in Cell Press, https://www.cell.com/).

1.1.1 Nociception

To investigate pain, it is necessary to clearly differentiate it from nociception, a term first introduced by Sherrington (1900) and now defined as "the neural process of encoding noxious stimuli" (Merskey and Bogduk, 1994). Nociception is a subconscious process which is driven by nociceptors, specialized sensory neurons, and is not to be confused with pain, a conscious experience. Nociceptors are differentially and specifically activated by noxious stimuli and consist of two major types: the medium diameter myelinated Aδ, mediating well-localized fast pain, and the small diameter unmyelinated C fibers, mediating poorly localized slow pain. Both types of nociceptors transmit nociceptive signals to the dorsal horn of the spinal cord, where they are synaptically connected to second-level neurons which predominantly project to the

thalamus and brainstem via the spinothalamic and spinoreticulothalamic tracts, respectively (Basbaum et al., 2009). From the thalamus and the brainstem, nociceptive information reaches the cerebral cortex where the transformation into a pain experience occurs. Notable brain regions include the somatosensory cortex, relevant for the sensory aspect, and the amygdala, relevant for the emotional aspect of unpleasantness (Corder et al., 2019). However, no brain area has been found to be solely, or even predominantly, responsible for pain (Apkarian et al., 2005; Baliki and Apkarian, 2015). Apart from the function of transmitting nociceptive information from the periphery to the brain, primary afferent nociceptor fibers show a special morphology called pseudo-unipolar, making them receptive to both ascending and descending information, i.e. nociceptors are bidirectional neurons (Basbaum et al., 2009). An illustration of the nociceptive pathway is shown in Figure 1.

While many pain experiences are preceded by nociception, it is important to note that nociceptive activity does not necessarily lead to pain perception, a phenomenon which is commonly observed in highly trained athletes, e.g. climbers who carry their complete body weight on just the tips of their fingers or toes for minutes to hours while reporting deep positive emotional satisfaction during an activity that continuously and massively activates their toe and finger nociceptors. Furthermore, nociceptive activity does not linearly translate into pain perception, i.e. a painful stimulus of identical intensity does not always elicit the same pain experience, which has been shown in many studies, even across species (Hu and Iannetti, 2019). Further, experiments in which participants received a controlled painful heat stimulus have shown that the perceived pain intensity significantly dissociates from the objective stimulus intensity after just a few minutes of stimulation (Schulz et al., 2015; Nickel et al., 2017). All of this indicates that the actual experience of pain is an integrative process which takes into account not just nociceptive information from afferent sensory neurons, but also the contextual information provided by concurrent emotional and cognitive processing (Ploner et al., 2017), something which is also reflected in the IASP's definition of pain.

1.1.2 Protective pain

Pain normally functions as a protective mechansim, warning the body of danger, disease or injury and is necessarily highly unpleasant and salient, steering attention, action and subsequent learning (Seymour, 2019). This pain can be nociceptive, i.e. evoked by potentially tissue-damaging mechanical, chemical or thermal stimuli. But it can also be inflammatory, caused by adaptive processes occurring after injury or infection to promote increased protection of the afflicted area. These adaptive processes are hyperalgesia (Hucho and Levine, 2007), an abnormally increased pain sensitivity, and allodynia (Latremoliere and Woolf, 2009), the experience of pain in response to innocuous stimuli such as a light touch. Being unable to experience this nociceptive or inflammatory pain has dire consequences, e.g. mutilation of the

extremities in individuals with congenital insensitivity to pain (Bennett and Woods, 2014) or severe damage to the joints in arthritis patients under strong analgesic medication (Denk et al., 2017), which indicates the essential role of pain in keeping the body safe from harm.

However, when pain persists beyond the tissue's healing time, it becomes pathological and loses its protective function. This is commonly called chronic pain. At the same time, the relationship between stimulus and resulting perception become intransparent. Nociceptive pain can be directly attributed to a brief noxious stimulus which results in a brief pain experience. Inflammatory pain is the result of a tissue damage, persisting until the damage has been healed and subsequently disappearing. However, chronic pain often persists past any externally observable effects of the tissue damage or external stimulus, making its treatment extremely challenging. An illustrative summary of these three kinds of pain is depicted in Figure 2. From a clinical point of view, acute and even inflammatory pain management is highly advanced and effective, and there exist a myriad of opioids and other analgesia which are routinely used to great effect, e.g. to reduce or even eliminate the pain of a surgical intervention, a pain that would be unimaginable and unbearable without analgesia. Therefore, the clinically more important research topic is the pathological, chronic pain, a disease in its own right.

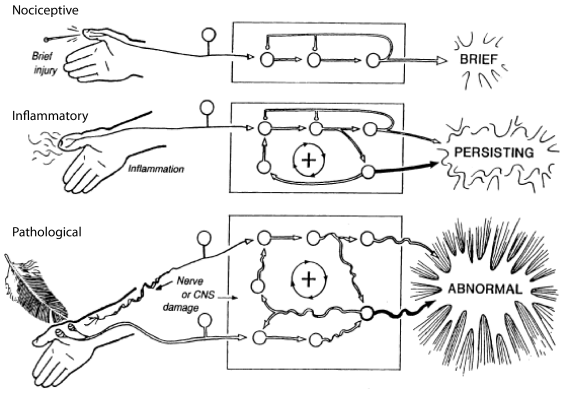

Figure 2: Three kinds of pain.

A simplified schematic of nociceptive, inflammatory and pathological pain. In this illustration the underlying mechanisms are represented as circuits, producing brief pain in response to a simple injury, persisting pain in response to an inflammation and abnormal pain as a consequence of damage to a nerve or the central nervous system (CNS). The pathological pain depicted here is a special form defined as neuropathic pain, caused by a lesion or disease of the somatosensory nervous system (Merskey and Bogduk, 1994). It should be noted that the actual relationships between stimuli and pain are in general far more complex. Adapted from Cervero and Laird (1991) with permission (originally published in News in Physiological Sciences, https://www.physiology.org/).

1.1.3 Chronic pain

Chronic pain is defined by the IASP as "pain that persists or recurs for longer than 3 months" (Treede et al., 2019). In addition to ongoing pain, chronic pain is a disease characterized by significant sensory, cognitive and affective abnormalities (Moriarty et al., 2011; Velly and Mohit, 2017), which have severe detrimental effects on quality of life. Affecting between 20 and 30 percent of the adult population (Breivik et al., 2006; Kennedy et al., 2014), chronic pain is a leading cause of disability worldwide (Rice et al., 2016). According to the Global Burden of Disease Study (2017), four out of the leading ten causes of years lived with disability are chronic pain afflictions

(Table 1). The World Health Organization (WHO) has also recently acknowledged this by including chronic pain as a health condition in its own right for the first time in the new edition of the International Classification of Diseases (ICD-11) (Treede et al., 2019). At the same time, its underlying pathology is not completely understood and current treatments of chronic pain often follow a trial-and-error strategy, with 40 percent of patients suffering from chronic pain reporting dissatisfaction with their care (Breivik et al., 2006). As the abuse of opioids worldwide, particularly in the United States where it is dubbed the "opiod crisis" (The Lancet, 2017), continues to be a significant problem for a large percentage of the population (Rudd et al., 2016; Koh, 2017; Rutkow and Vernick, 2017; The Lancet, 2017; Volkow and Collins, 2017) and the healthcare system, costing about 600 billion dollars per year in the USA (Institute of Medicine of the National Academies, 2011), alternatives to or improvements to pharmacological therapies would be a welcome addition to the arsenal of treatments against chronic pain. Thus, advances in the understanding and treatment of chronic pain are urgently needed.

Table 1: Leading ten causes of years lived with disability worldwide in 2016

1	2	3	4	5	6	7	8	9	10
Back pain	Migraine	Hearing	Iron	MDD	Neck pain	Oth MSK	Diabetes	Anxiety	Falls

Afflictions related to chronic pain are highlighted in red. Anxiety = Anxiety disorders. Back pain = Low back pain. Diabetes = Diabetes mellitus. Iron = Iron-deficiency anaemia. MDD = Major depressive disorder. Oth MSK = Other musculoskeletal disorders. Adapted from the Global Burden of Disease Study (2017).

Chronic pain is generally associated with two mechanisms of sensitization: peripheral and central sensitization. In the periphery, tissue damage often results in synthesis and accumulation of the so-called "inflammatory soup", a wide array of signaling molecules, e.g. neurotransmitters, released from activated nociceptors or non-neural cells in the local area of the injury. Excitability of nociceptors in this area is subsequently enhanced, resulting in the increased sensitivity to temperature and touch (Julius and Basbaum, 2001; Basbaum et al., 2009). At the level of the spinal cord, numerous processes occur concurrently to cause central sensitization, a state of hyperexcitability in response to nociceptive signals. Among these processes are enhancement of glutamatergic neurotransmission, loss of inhibitory control, and microglia activation (Scholz and Woolf, 2002; Basbaum et al., 2009). A common mechanism of these processes is the enhancement of afferent nerve fiber sensitivity along the nociceptive pathway. Though the peripheral and central sensitization are very well-studied and their molecular mechanisms have been understood to a great extent, they can only explain the sensory aspect of chronic pain. It has become clear that purely treating the site of injury is often not enough to completely cure the patient of their pain. Lower back pain is one of the most common pain afflictions, yet the chances of becoming pain-free after chronic pain onset are less than 50 percent with the current clinical care (Vingard et al., 2002; Henschke et al., 2008; Costa Lda et al., 2009). It is therefore imperative to look beyond the current standard of only treating the injured site and towards potential treatment options based on cognitive mechanisms.

1.1.4 The role of the brain in experimental pain

Pain is the result of interactions between sensory and contextual (i.e. cognitive, emotional and motivational) processes (Melzack and Casey, 1968). As mentioned above, the mechanisms of both acute and persistent pain have been extensively investigated on the level of the periphery and the spinal cord. However, the contextual processes and the integration of the sensory and contextual information, both of which are high-level processes mainly occuring in higher brain regions (Bushnell et al., 2013) such as the cerebral cortex, have only recently shifted into the focus of pain research. Studies in animals and humans have revealed a robust activation of an extended network of brain areas in response to experimentally inflicted acute pain. The most consistently activated regions constitute the so-called "pain matrix" and include the somatosensory, insular, cingulate and prefrontal cortices, as well as the thalamus, basal ganglia, cerebellum and amygdala (Peirs and Seal, 2016). However, it has not been shown that the activation of this pain matrix specifically represents pain (Legrain et al., 2011). Rather, it has become clear that pain has to be represented by a dynamic pain connectome (Kucyi and Davis, 2015), a neural signature for pain with both spatial specificity and temporal dynamics.

In studies investigating the temporal and spectral patterns of brain activity with electrophysiological recordings such as EEG and magnetoencephalography (MEG), experimental acute pain has been associated with specific spatial-temporal-spectral responses (Ploner and May, 2018). Most commonly studied in the context of acute experimental pain is a typical sequence of responses evoked by brief noxious stimuli, termed N1, N2, and P2 responses, see Figure 3. These originate mainly from the somatosensory, insular, and cingulate cortices (Garcia-Larrea et al., 2003). These responses are correlated with nociceptive pathway damage, stimulus intensity, subjective pain perception, attention and cognitive modulations, but are not specific to pain (Ploner and May, 2018). Instead, they mostly reflect the salience of these noxious stimuli (Mouraux and Iannetti, 2009; Mouraux et al., 2011). In addition to these time-locked evoked responses, time-frequency analyses have shown modulations of neural oscillations at alpha (8 - 13 Hz), beta (13 - 30 Hz), and gamma (40 -100 Hz) frequencies (Gross et al., 2007; Schulz et al., 2011; Zhang et al., 2012) in response to brief noxious stimuli, which are also modulated by contextual factors (Tiemann et al., 2015). In an effort to more closely model the more clinically relevant chronic pain, some studies have used a tonic pain paradigm, extending the duration of the afflicted experimental pain from the range of (milli-) seconds to minutes. These studies have shown an association of tonic pain with a suppression of neural oscillations at alpha (Nir et al., 2012; Nickel et al., 2017; Li et al., 2016; Schulz et al., 2015) and beta (Nickel et al., 2017) frequencies. Further, several studies have found increased gamma oscillations during tonic pain stimulation (Peng et al., 2014; Nickel et al., 2017). Intriguingly, this increase was localized to the medial prefrontal cortex instead of sensorimotor areas (Nickel et al., 2017). Whether these effects are specific

to pain is of yet unclear, however, as e.g. most mental processes also suppress alpha oscillations (Ploner et al., 2017).

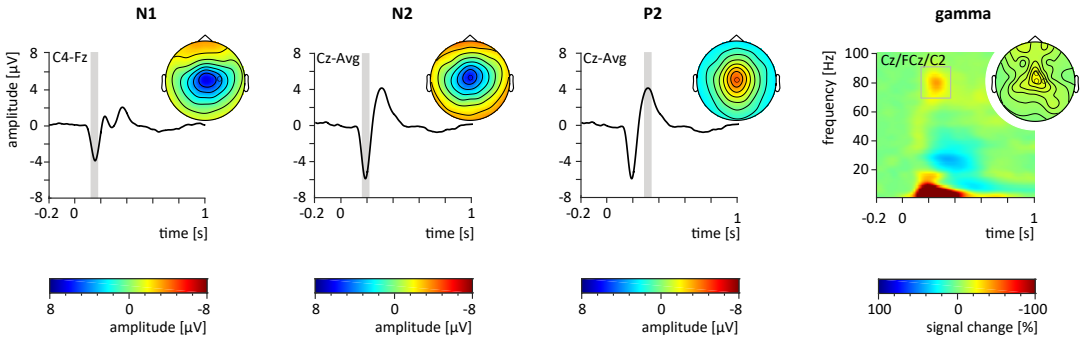

Figure 3: Electrophysiologically recorded brain responses to brief noxious stimuli.

Mean time courses and time-frequency representation (TFR, right-most panel) of EEG brain responses to approximately 180 brief painful laser stimuli applied to the left hand, averaged across 51 participants. Marked time periods and time-frequency windows indicate periods chosen to quantify N1, N2, P2, and gamma responses, in this study motivated by previous literature. Topographies depict the scalp distribution of neural activity in these periods, electrodes used for the quantification of the different responses are marked. The TFR is displayed as percent-signal change relative to a prestimulus baseline (- 1000 to 0 ms). Reproduced from Tiemann et al. (2018) with permission (originally published in Nature Communications, https://www.nature.com).

In summary, experimental pain has been shown to be represented by a complex spatial, temporal and spectral pattern of brain activity which shows a remarkable lack of specificity in its spatial and spectral dimensions, in the sense that activity at a single location or frequency is not completely predictive of the pain experience. It has instead become clear that multiple aspects of brain activity collaborate to form a complex pattern of neural activity to eventually determine the subjective pain experience in an experimental setting. Further basic research on the processing of experimental pain could facilitate understanding the dysfunctional alterations which lead to chronic pain by providing a template of healthy pain processing.

1.1.5 Alterations of the brain in chronic pain

Studies in animals and humans have revealed that chronic pain is associated with significant structural and functional changes of the brain (Baliki and Apkarian, 2015; Rauschecker et al., 2015; Kuner and Flor, 2017). Not only have somatosensory and motor areas been associated robustly with chronic pain (Ploner and May, 2018; Mouraux and Iannetti, 2018), but also the prefrontal cortex and subcortical brain areas including amygdala, hippocampus, insula and striatal areas have been implicated in chronic pain (Hashmi et al., 2013; Baliki and Apkarian, 2015; Rauschecker et al., 2015; Vachon-Presseau et al., 2016; Kuner and Flor, 2017; Seminowicz and

Moayedi, 2017; May et al., 2018; Corder et al., 2019). An illustrative summary of brain changes found to be associated with chronic pain is shown in Figure 4.

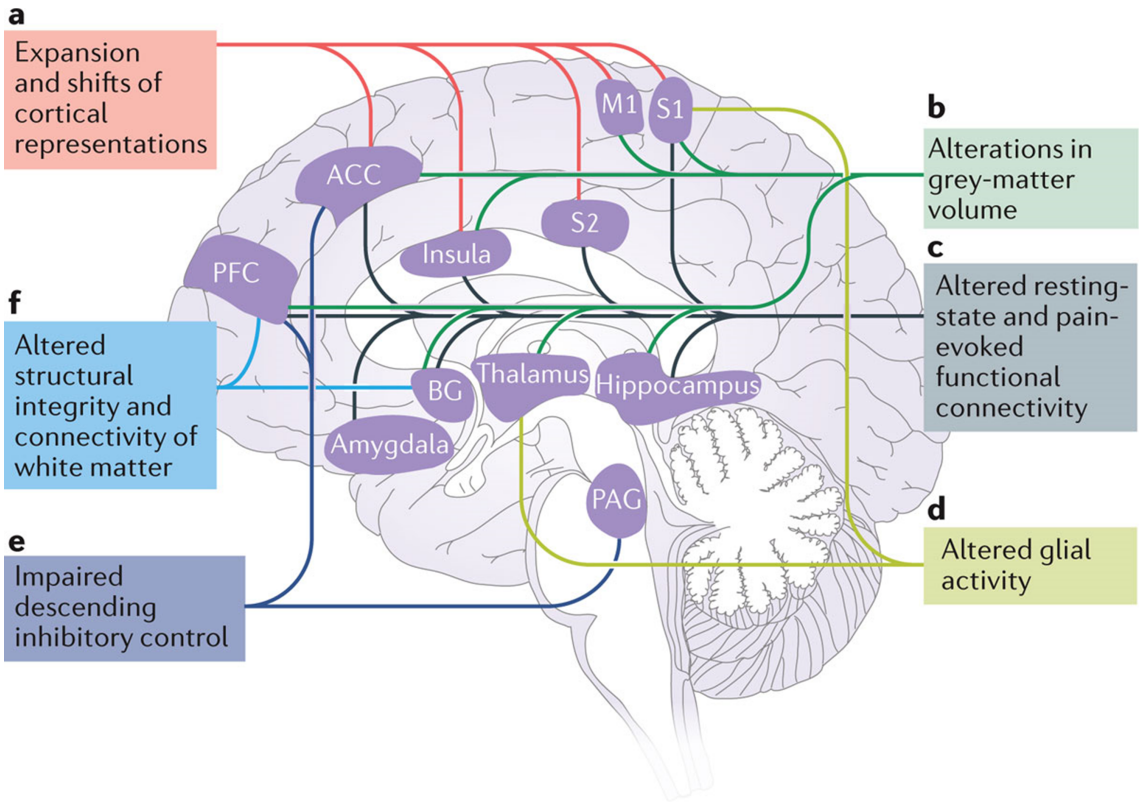

Figure 4: Structural and functional changes in the human brain in chronic pain conditions.

a | Brain areas undergoing functional reorganization. **b** | Regions of grey-matter alterations. **c** | Altered resting-state and pain-evoked functional connectivity. **d** | Brain glial activation. **e** | Changes in activity in descending inhibitory pathways. **f** | Changes in white-matter integrity and structural connectivity. ACC, anterior cingulate cortex; BG, basal ganglia; M1, primary motor cortex; PAG, periaqueductal grey; PFC, prefrontal cortex; S1, primary somatosensory cortex; S2, secondary somatosensory cortex. Reproduced from Kuner and Flor (2017) with permission (originally published in Nature Reviews Neuroscience, https://www.nature.com).

Structurally, alterations in both grey and white matter have been observed in patients suffering from chronic pain. Grey matter atrophy was mainly found to affect the insula (Geha et al., 2008), cingulate (Schmidt-Wilcke et al., 2006), thalamus and prefrontral cortex (Apkarian et al., 2004); see May (2008) for a review. In some cases, successful analgesic treatment of chronic pain even led to the reversal of grey matter changes in the prefrontal cortex (Seminowicz et al., 2011). Further, alterations in white matter structure especially in prefrontal areas (Mansour et al., 2013) and corticolimbic regions (Vachon-Presseau et al., 2016) have been associated with the transition from acute pain to chronic pain, representing putative anatomical risk factors for pain chronification.

Functionally, Hashmi et al. (2013) observed that conversion from subacute to chronic back pain was accompanied by a shift of brain activation patterns from somatosensory (S1 and S2) and motor regions (M1), which are robustly involved in processing of brief experimental pain, to regions commonly associated with emotional processing, i.e. the insula, medial prefrontal cortex (mPFC), anterior cingulate cortex (ACC), and the amygdala. Intriguingly, this shift of cortical representation is also observed in tonic experimental pain application within a few minutes of stimulation (Nickel et al., 2017; Schulz et al., 2015), albeit less pronounced. FMRI studies investigating functional connectivity at rest have shown disruptions in the so-called default mode network (Baliki et al., 2008), a resting-state network which is robustly activated in task-free fMRI recordings and is mainly comprised of the medial prefrontal cortex, the cingulate cortex, the lateral temporal cortex, the inferior parietal lobe, and the hippocampus (Buckner et al., 2008). The default mode network is associated with self-reflection and mind-wandering (Buckner et al., 2008) and often implicated in neurological conditions with cognitive impairments, such as Alzheimer's disease (Badhwar et al., 2017), or psychotic forms of schizophrenia (Baker et al., 2019). Only few EEG and MEG studies have investigated the brain activity of patients suffering from chronic pain and the results have been heterogeneous. A few studies have observed increased theta (4 - 8 Hz) frequency power and/or a lowered peak frequency at rest in these patients (Llinas et al., 1999; Sarnthein et al., 2006; Stern et al., 2006; Vuckovic et al., 2014; Meneses et al., 2016; Di Pietro et al., 2018; Fallon et al., 2018; Vanneste et al., 2018). These findings have been related to the Thalamocortical Dysrhythmia (TCD) model of chronic pain (Llinas et al., 2005). In this model, abnormal nociceptive input causes abnormal thalamic bursts at theta frequencies. These theta oscillations are transmitted to the cerebral cortex, where they result in disinhibition of neighboring areas, which, in turn, results in abnormal oscillations at gamma ($>$ 30 Hz) frequencies and eventually in ongoing pain. This model is highly appealing, but evidence is still sparse. Just as many studies, if not more, were unable to reproduce these findings (Boord et al., 2008; Walton et al., 2010; Schmidt et al., 2012; de Vries et al., 2013; van den Broeke et al., 2013; Gonzalez-Roldan et al., 2016; Gonzalez-Villar et al., 2017; Vanneste et al., 2017). The main issues contributing to the uncertainty of these results are most likely the limited sample sizes - most of these studies involved fewer than 20 patients - coupled with the publication towards positive findings which pervades most scientific fields (Baker, 2016). Further insights into the brain mechanisms of chronic pain not only promise to advance the understanding of the underlying pathophysiology, but could also be highly useful in a clinical setting. In particular, a brain-based marker of pain could be immensely helpful for the diagnosis and treatment of pain (Davis et al., 2017; Upadhyay et al., 2018). EEG in particular, which is capable of capturing the fast temporal patterns of brain activity, shows exceptional potential for developing such a marker.

1.2 Fundamentals of EEG for Pain Research

An extensive characterization of EEG (Buzsaki, 2006; Nunez and Srinivasan, 2006; Kandel, 2013) is beyond the scope of this dissertation. However, a few relevant properties will be listed and discussed in the following. On the one hand, the biggest advantage of EEG over other techniques of non-invasive functional neuroimaging such as Positron Emission Tomography (PET) and fMRI is EEG's temporal resolution. EEG can capture brain activity in the range of milliseconds, whereas PET and fMRI have a latency of several seconds. On the other hand, EEG's biggest weakness is its spatial resolution. Localizing sources to within a cube of 1 cm^3 is already at the theoretical limit for EEG data, even with high-density recording systems (Nunez and Srinivasan, 2006). Further, sub-cortical regions such as the insula or amygdala contribute very little to the overall EEG signal, resulting in a low signal-to-noise ratio in deep brain structures (Seeber et al., 2019).

1.2.1 The neurophysiological basis of EEG

The human brain consists of about 86 billion neurons, of which about 19 per cent, i.e. about 16 billion, are situated in the cerebral cortex (Azevedo et al., 2009). Every neuron generates time-varying electrical currents when activated: the action potential, mediated by sodium and potassium ion flow, and the postsynaptic potential, mediated by synaptic activation which is in turn mediated by neurotransmitter systems (da Silva, 2009). From the brain's neurons, these electric currents propagate to the surface of the scalp via volume conduction, where they can be recorded using non-invasive electrodes. It is important to note that the main contributors to the measured signal are neurons that form a so-called "open field" (Lorente de No, 1947), a geometric configuration of the neurons in which the dendrites face one direction and the soma face another. This leads to the generation of a strong superimposed dipole in the case of synchronous acti-

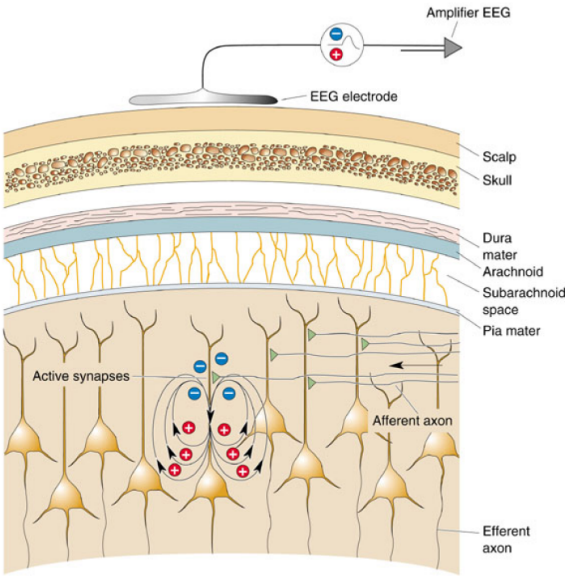

Figure 5: The postsynaptic potential.

The schematic depicts a model of the electric dipole formed by pyramidal neurons in the cortex which are the basis of the EEG signal measured at the scalp. It also shows the many layers of organic tissue separating the electrodes recording the electrical brain activity from the sources generating it. Note the "open field" configuration of the neurons, with the apical dendrites aligned perpendicularly to the cortical surface and therefore also to the EEG electrode. Reproduced from Bear et al. (2016) with permission (originally published by Wolters Kluwer Health, https://shop.lww.com).

vation of the dendrites, and is mainly found in pyramidal neurons of the cortex (Okada et al., 1997; Murakami and Okada, 2006). Thus, at its core, EEG is a measurement of the synchronized electric activity created by neural activity of a population of neurons, mainly from the cerebral cortex. Each EEG electrode picks up the activity of many thousands to millions of neurons from all over the head and even from the neck, not only of the neural populations directly beneath the electrode. This explains the spatial unspecifity of EEG. A neural population's electrical activity is directly linked to information transfer between neurons and EEG is easily able to sample this electrical activity at 1000 Hz or more, therefore offering insights into macro-level information transfer at high temporal resolution. This temporal resolution is important for investigations of the brain responses to external stimuli (typically showing latencies of at least 100 ms depending on the location and modality of the stimulus (e.g. Gross et al. (2007)) or inter-regional communication in the brain.

1.2.2 Evoked and induced brain activity in experimental pain

EEG studies have mostly investigated either the event-related potentials (ERP), "voltage fluctuations in the EEG that are time-locked to internal or external events (e.g. stimuli, responses, decisions)" (Luck et al., 2011), or neural oscillations, which can be induced by external stimuli but also occur intrinsically in the human brain.

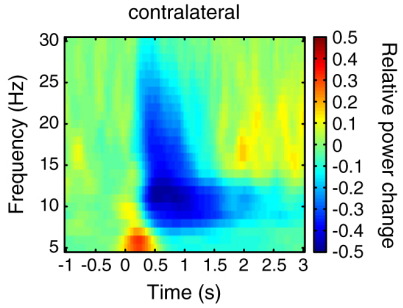

Figure 6: Pain-induced alpha and beta frequency repsonses

Average time-frequency responses over right temporal channels to contralateral hand stimulation by a laser, averaged over 15 subjects. Power changes relative to a pre-stimulus baseline (-1 to 0 seconds relative to stimulus onset) are color-coded. Adapted from May et al. (2012) with permission (originally published by Elsevier, https://www.elsevier.com).

Most studies investigating brain responses to experimental pain in humans have investigated responses to a brief painful stimulus (Ploner and May, 2018). A common experimental brief painful stimulus is the application of a laser pulse onto the skin. This type of stimulation offers a brief (milliseconds) stimulus which selectively activates nociceptors without co-activating tactile sensory fibers (Plaghki and Mouraux, 2005). Typically, laser stimuli applied to the hand dorsum robustly elicit a triphasic sequence of temporal responses (see Figure 3): first, a small negative deflection of the EEG activity is observed at contralateral temporal electrodes, peaking approximately 170 ms after stimulus application (N1). After the N1 response, EEG activity at central electrodes shows another large negative deflection, peaking approximately 250 ms after stimulus application (N2), followed immediately by a large positive deflection which peaks approximately 390 ms after stimulus application (P2) (Plaghki and Mouraux, 2005). These brain responses to laser stimuli are known as laser-evoked potentials (LEP), a subtype of ERPs, and have been established as a clinical tool

to measure integrity of nociceptive pathways (Ploner and May, 2018), and as a research tool to study basic pain perception and various modulations such as attention (Legrain et al., 2009) or placebo effects (Tiemann et al., 2015).

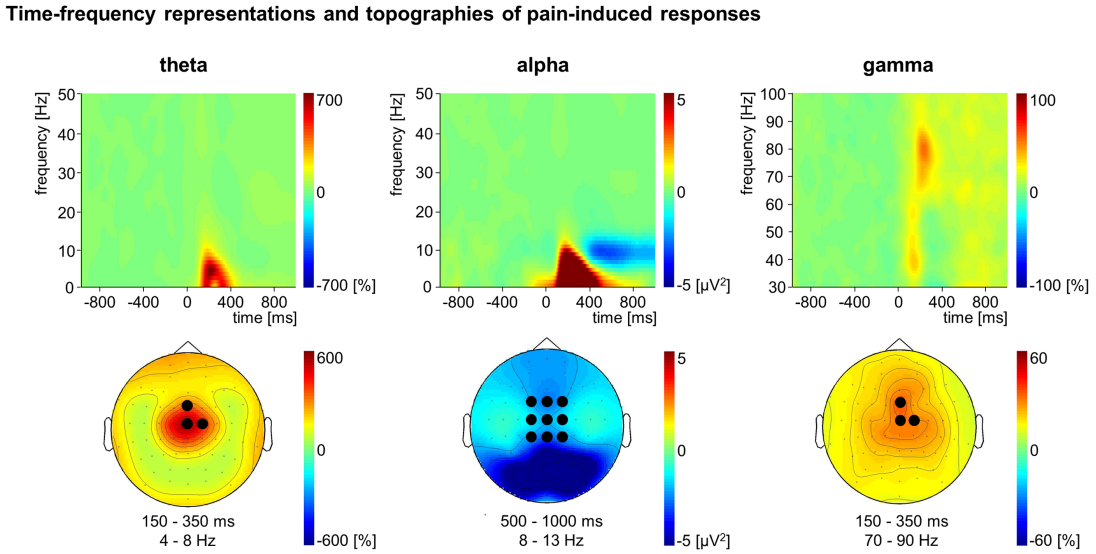

Figure 7: Pain-induced neuronal responses in the theta, alpha, and gamma frequency bands.

The upper row shows time–frequency representations of neuronal activity in response to painful stimulation as compared to a prestimulus baseline (2800 to 200 milliseconds) averaged across 20 subjects. Responses were averaged across central electrodes as marked in the corresponding topographical maps of theta, alpha, and gamma responses in the lower row. TFRs and topographies illustrating gamma and theta responses are displayed as percent signal change relative to baseline, whereas those illustrating alpha responses are displayed in absolute power minus baseline power. TFR, time–frequency representation. Reproduced from Tiemann et al. (2015) with permission (originally published by Wolters Kluwer Health, https://shop.lww.com).

Experimental pain further induces modulations of neural oscillations in four frequency bands (see Figure 6 and Figure 7): theta (4-8 Hz), alpha (8-13 Hz), beta(14-30 Hz), and gamma (30-100 Hz). Neural oscillations are periodic oscillations which are robustly and ubiquitously observed in EEG. The underlying mechanisms of these oscillations are challenging to explain as they diverge substantially from the invasive single-unit recordings which have been obtained in recent years (Cardin et al., 2009; Womelsdorf et al., 2014). This can partly be explained by the fact that the signal recorded at the scalp by EEG electrodes is a superposition of millions of neurons and neural cell assemblies. There exist models on a microscopic scale such as the Hodgkin-Huxley model (Hodgkin and Huxley, 1952) for single neuron activity, modeling every component of a single cell as an electrical element, and there exist models on a macroscopic scale such as the Kuramoto model (Kuramoto, 1975), describing the brain as a system of coupled oscillators leading to synchrony and subsequent large-scale oscillations. But creating a model which accurately spans the gap from single neuron activity to macro-scale phenomena has been challenging. Though no general theory for the generation and function of neural oscillations has yet been

established, it has become clear that neural oscillations are an essential property of neural networks. One of the most compelling theories concerning the function of brain oscillations is the so-called communication-through-coherence theory (Fries, 2015). The theory states that a neural assembly tends to synchronize rhythmically, creating temporal windows of high and low postsynaptic excitability. Thus, postsynaptic neuronal groups which receive inputs from multiple presynaptic neuronal groups would preferably respond to the coherent presynaptic groups. Further, communication with inputs which consistently and repeatedly arrive in coherent windows would be enhanced. In other words, the theory proposes a postsynaptic amplifying multiplexing via oscillations.

Brief noxious stimuli induce increased activity in the theta frequency band between 150 and 400 ms after stimulus onset, which strongly overlaps with pain-evoked ERP responses (Tiemann et al., 2018; Ploner et al., 2017). Transient suppression of alpha and beta frequencies can be observed both in phasic (May et al., 2012) and tonic pain paradigms (Nickel et al., 2017), where they have been shown to more closely reflect the stimulus intensity than the perceived pain (Schulz et al., 2015; Tiemann et al., 2015; Nickel et al., 2017). Phasic pain stimuli also induce gamma frequency oscillations over the sensorimotor cortex between 150 to 350 ms after stimulus onset (Gross et al., 2007; Hauck et al., 2007; Ploner et al., 2006). Interestingly, in tonic pain the induced gamma frequency oscillations have been observed to shift from the sensorimotor cortex to the medial prefrontal cortex (Nickel et al., 2017). The induced gamma frequency oscillations have been shown to correlate with the reported pain intensity, not just the objectively applied stimulus intensity (Gross et al., 2007; Zhang et al., 2012; Nickel et al., 2017). However, different pain perception modulations (e.g. via attention) affect the induced neural oscillations differentially (Ploner et al., 2017), making a precise assignment of a neural oscillation to a function difficult, and indicating, as mentioned in subsection 1.1.4, that there is no direct correspondence between a certain neural oscillation and pain, but rather an unspecific relationship. However, it has become clear that longer-lasting pain does not simply lead to continued signaling of acute pain, but that processing already shifts after a few minutes of tonic pain (Nickel et al., 2017), implying even greater changes in chronic pain, which lasts for months, years, or even decades.

1.2.3 Spontaneous brain activity at rest in chronic pain

For a long time, recordings of brain activity without any task were thought to contain little to no information, and were mostly used as a control condition for task-based experiments. But recent observations of this so-called resting-state have shown that robust and meaningful brain activity can be observed (Damoiseaux et al., 2006; Fox and Raichle, 2007). Beyond the maintenance of normal bodily functions, mind-wandering, self-reflection, and similar cognitive processes are a common occurrence during prolonged task-free periods (Buckner et al., 2008). Further, abnormalities

of brain activity during resting-state recordings, as measured by several recording techniques such as PET, fMRI and MEG or EEG, have been reliably linked to pathological neurological conditions such as Alzheimer's disease (Badhwar et al., 2017), Parkinson's disease (Politis, 2014), or schizophrenia (Baker et al., 2019).

Patients with chronic pain regularly suffer from pain without experiencing any noxious external stimuli, often reporting spontaneous pain attacks or a constant level of pain. This is the basis for the hypothesis that differences of brain activity between chronic pain patients and healthy controls without pain should be observable even during periods without any particular task or stimulus. As discussed in 1.1.5, fMRI studies have robustly shown alterations in functional connectivity in chronic pain patients at rest. To translate these observational results into a clinically useful tool, recent fMRI studies have tried to establish an objective, brain-based marker of experimental (Wager et al., 2013) and chronic pain (Mansour et al., 2016; Mano et al., 2018). Accordingly, the feasibility, limitations and perspectives of brain-based markers of pain are currently the subject of intensive discussion in the pain research community (Rosa and Seymour, 2014; Hu and Iannetti, 2016; Davis et al., 2017; Smith et al., 2017; Upadhyay et al., 2018) and beyond (Reardon, 2015; Makin, 2016; Woo et al., 2017a).

1.3 The Search for a Marker of Chronic Pain

A joint working group of the US Food and Drug Administration (FDA) and the National Institutes of Health (NIH) defined a biomarker as a "defined characteristic that is measured as an indicator of normal biological processes, pathogenic processes, or responses to an exposure or intervention, including therapeutic interventions" (FDA-NIH Biomarker Working Group, 2016). The potential uses for a biomarker of pain are illustrated in Figure 8, and, with the exception of those relating to animals and anaesthetised patients, all of them apply to a brain-based marker of chronic pain as well. In the following, the term "pain biomarker" is avoided as the definition of "biomarker" includes the following passage: "A biomarker is not an assessment of how an individual feels, functions, or survives" (FDA-NIH Biomarker Working Group, 2016), which stands in direct contrast with the definition of pain. However, any kind of pain marker is unlikely to replace the current gold standard for pain assessment, a self-report by the patient (Davis et al., 2017; Mouraux and Iannetti, 2018; Tracey et al., 2019). A marker would instead supplement self-reports and enable better informed prognoses. Furthermore, differential diagnoses of the various types of chronic pain could be supported by a physiological and objective diagnosis criterion, as criteria for differential diagnoses of some pain disorders can be vague. As an example, fibromyalgia, a subtype of chronic widespread pain, is typically diagnosed through exclusion of other pain disorders (Clauw, 2014). A correct differential diagnosis is directly linked with another use of a brain-based marker: treatment of chronic pain. As in many other diseases for which a biomarker has already been established, treatment of chronic pain could be optimized by evaluating changes of the marker as a proxy for the severity of the disease, thereby guiding treatment efforts. This would be especially useful for e.g. pharmacological interventions, which can have severe side effects.

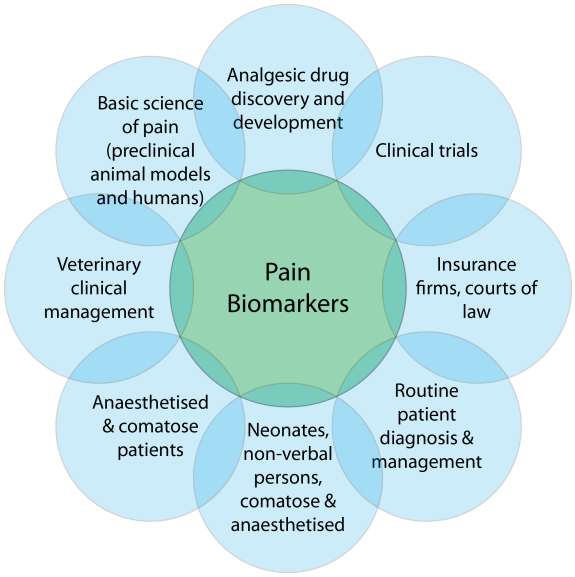

Figure 8: Potential uses for a pain biomarker.

Reproduced from Tracey et al. (2019) with permission (originally published in Cell Press, https://www.cell.com/).

In 2017, an international task force of influential pain researchers defined the following 7 criteria that a neuromarker of pain based on neuroimaging should ideally fulfill (Davis et al., 2017):

1. A precise definition of a pain neuromarker.
2. Applicability of the pain neuromarker to individuals.

3. Methodological procedures used during testing must be validated.
4. Measures must be internally consistent and image data quality validated for the individual tested using positive and negative controls.
5. The neuromarker must be diagnostic for pain.
6. The neuromarker must be validated with converging methods.
7. The neuromarker must be generalizable to the patient group tested and to the test conditions.

At the same time, the task force's consensus was that "current brain-based measures fall short of the requisite standards" (Davis et al., 2017). Several fMRI studies have tried establishing a neuromarker of pain, the most noteworthy of which is the so-called Neurologic Pain Signature (NPS) (Wager et al., 2013). The NPS is a weighted activation map outputting a single value at any time point, predicting the perceived pain of the recorded person at that time. The NPS was developed to predict pain experience but suffers from its insensitivity to psychological interventions such as placebo treatment (Woo et al., 2017b). Refer to Figure 9 for a thresholded map of the NPS.

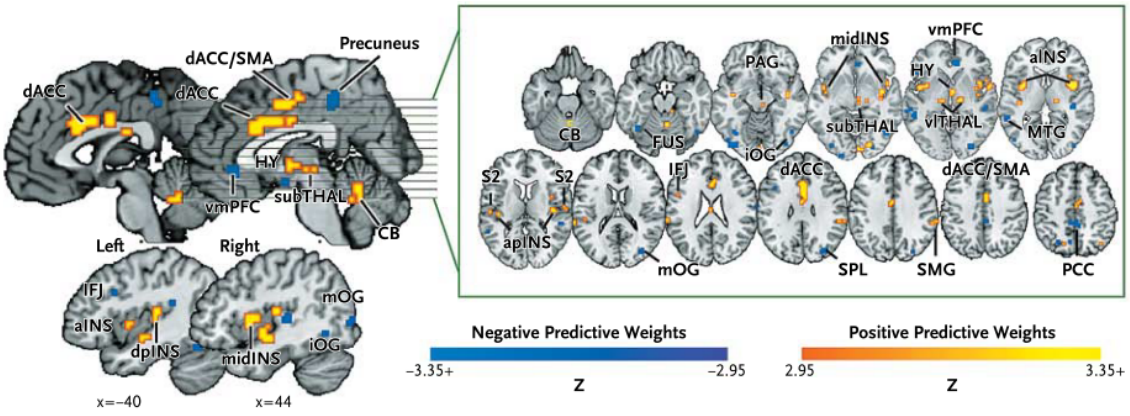

Figure 9: The Neurologic Pain Signature (NPS).

The figure shows the neurologic pain signature for fMRI as proposed by Wager et al. (2013), consisting of voxels in which activity reliably predicted pain. The map shows weights that exceed a threshold (a false discovery rate of q<0.05) for display only; all weights were used in prediction. ACC denotes anterior cingulate cortex, CB cerebellum, FUS fusiform, HY hypothalamus, IFJ inferior frontal junction, INS insula, MTG middle temporal gyrus, OG occipital gyrus, PAG periaqueductal gray matter, PCC posterior cingulate cortex, PFC prefrontal cortex, S2 secondary somatosensory cortex, SMA supplementary motor area, SMG supramarginal gyrus, SPL superior parietal lobule, TG temporal gyrus, and THAL thalamus. Direction is indicated with preceding lowercase letters as follows: a denotes anterior, d dorsal, i inferior, l lateral, m middle, mid mid-insula, p posterior, and v ventral. Reproduced with permission from Wager et al. (2013), Copyright Massachusetts Medical Society.

As a potential first step towards an EEG marker of chronic pain, some EEG studies have shown a slowing of neural oscillations together with an increase of oscillatory brain activity at theta frequencies in chronic pain patients (Sarnthein et al., 2006; Vanneste et al., 2018). These observations have been embedded in the

Thalamocortical Dysrhythmia (TCD) model of neuropsychiatric disorders (Llinas et al., 2005). In this model, abnormal nociceptive input causes abnormal thalamic bursts at theta frequencies. These theta oscillations are transmitted to the cerebral cortex where they result in disinhibition of neighboring areas, which, in turn, results in abnormal oscillations at gamma frequencies and eventually in ongoing pain. This model is highly appealing, but evidence is sparse, contradictory, and mostly confined to small groups of patients suffering from neuropathic subtypes of chronic pain (see Pinheiro et al. (2016) or 1.1.5 for a review). Thus, a general EEG-based marker of chronic pain remains to be demonstrated.

Using EEG to assess abnormalities of brain function and to establish a brain-based marker of chronic pain is particularly appealing as it is safe, non-invasive, cost-effective, broadly available and potentially mobile. EEG is not known to be associated with any side effects except for slight abrasion of the skin during preparation and has no contraindications. Additionally, the high temporal resolution of EEG enables online decoding and precise attribution of external stimulations, creating easily accessible feedback for novel manipulations of brain activity such as neurofeedback (Sitaram et al., 2017) or non-invasive brain stimulation techniques (Polania et al., 2018). Both techniques are, at their current state of research, based on altering brain activity in a spatially unspecific manner, i.e. it is currently not possible to precisely control the location of stimulation (Polania et al., 2018). At the same time, especially for neurofeedback, having a high temporal resolution for immediate feedback about changes in brain activity is likely to be crucial for these methods. For these reasons, an EEG-based target for manipulation appears very appealing, as EEG's greatest weakness, spatial inaccuracy, is less relevant, and its greatest strength, high temporal resolution, can be exploited.

1.4 Aims and Outline

In the present study, we aimed to harness the potential of EEG to determine abnormalities of resting-state brain activity as a potential brain-based marker of chronic pain. We therefore recorded resting-state data in a large cohort of chronic pain patients and age and gender-matched healthy controls. We then systematically analyzed global, i.e. spatially holistic, and local, i.e. spatially specific, measures of oscillatory brain activity, including all commonly used analyses of EEG data on resting-state data. Moreover, we performed connectivity analyses using phase and amplitude-based measures in source space as well as graph theory-based network analyses. A few studies have previously investigated EEG or MEG-based functional connectivity in chronic pain (Sarnthein and Jeanmonod, 2008; Gonzalez-Villar et al., 2017; Vanneste et al., 2017; Choe et al., 2018; Lee et al., 2018). However, to the best of our knowledge the present study is the first study to report a rigorously data-driven and whole-brain approach. In this univariate approach, we statistically compared the above mentioned measures between patients and healthy controls, strictly correcting for multiple comparisons. Our main hypothesis was explorative and simple: the brain activity and/or functional connectivity differs between chronic pain patients and matched healthy controls.

As discussed in 1.1.4 and 1.1.5, pain processing is likely to be represented by complex spatial, temporal, and spectral patterns of brain activity instead of measures of a single dimension. Thus, to further investigate not just single measures, but patterns of brain measures, we used a multivariate machine learning approach based on a support vector machine (SVM) to distinguish between chronic pain patients and healthy controls. This approach also enabled us to predict whether a person was part of the patient group or the healthy control group on an individual level, expanding the group-level contrast to a single-subject prediction. A comprehensive overview of the measures that were investigated is shown in Figure 12. The main hypothesis for our multivariate approach was therefore expanded: there is a pattern of brain activity and/or functional connectivity which differentiates between chronic pain patients and matched healthy controls.

Thus, we recorded the resting-state EEG of a large cohort of patients suffering from various types of chronic pain, and a matched cohort of healthy controls without pain. We systematically analyzed these recordings, contrasting the patients' data with the data of the healthy controls. Most of the following methods and the main results are part of another manuscript (Ta Dinh et al., Pain, in press); this secondary publication also shows supplementary material and control analyses that were not visualized or not described in detail in the original publication.

2 Material and Methods

2.1 Participants

101 patients (age 58.2 ± 13.5 years (mean ± standard deviation), 69 female) suffering from chronic pain of various types and 84 age and gender-matched healthy control participants (age 57.8 ± 14.6 years (mean ± standard deviation), 55 female) participated in the study. Inclusion criteria for patients were a clinical diagnosis of chronic pain, with pain lasting at least 6 months and a minimum reported average pain intensity $\geq 4/10$ during the last 4 weeks (0 = no pain, 10 = worst imaginable pain). Exclusion criteria were acute changes of the pain condition during the last 3 months, for example due to recent injuries or surgeries. Further exclusion criteria were major neurological diseases such as stroke, epilepsy or dementia, major psychiatric diseases aside from depression and severe general diseases. Finally, patients on medication with benzodiazepines, which have known effects on EEG signals (Bauer and Bauer, 2011), were excluded; other medications were not restricted. See Table 2 for group summaries of the patient and control cohort. Table 3 lists detailed patient characteristics. In summary, we included 47 patients with chronic back pain, 30 patients with chronic widespread pain, 6 patients with joint pain, 5 patients with unspecific neuropathic pain, 7 patients with post-herpetic neuralgia and 6 patients with poly-neuropathic pain. Exclusion criteria for healthy controls were a medical history of any chronic pain afflictions, any current painful injuries, major neurological diseases, and medication with benzodiazepines. All participants gave written informed consent. The study was approved by the ethics committee of the Medi-

Table 2: Demographics and questionnaire results.

	CP (N = 101, mean ± sd)	HC (N = 84, mean ± sd)
Gender (M/F)	32/69	29/55
Age	58.2 ± 13.5	57.8 ± 14.6
VR-12 PCS score	31.7 ± 7.8	52.74 ± 5.7
VR-12 MCS score	46.4 ± 12.0	54.1 ± 9.0
Curr. pain intensity (VAS)	5.2 ± 1.9	-
Avg. pain intensity (VAS)	5.7 ± 1.6	-
Pain duration (months)	121.9 ± 114.3	-
PDI score	28.3 ± 14.7	-
PDQ score	17.4 ± 6.5	-

CP, chronic pain patients; HC, healthy controls; VR-12, Veteran's RAND 12; PCS, physical component score; MCS, mental component score; Curr. pain intensity, currently experienced pain intensity; VAS, visual analog scale; Avg. pain intensity, average pain intensity in the last 4 weeks; PDI, pain disability index; PDQ, painDETECT.

cal Faculty of the Technische Universität München and carried out in accordance with the relevant guidelines and regulations. A power analysis for non-parametric t-tests using G*Power showed that the number of participants allowed for detecting differences between groups of at least medium effect size (Cohen's d $\geq$ 0.5) with a statistical power of 0.9.

Table 3: Patient characteristics.

ID	Age (ys)	Sex	Pain duration (months)	Curr. pain (VAS)	Avg. Pain (VAS)	Pain diagnosis	MQS	BDI	PDQ
1	67	m	360	5	5	CBP	4	3	30
2	54	f	120	4	5	CBP	32	35	14
3	64	f	96	5	7	CBP	11	7	16
4	41	m	24	7	6	CBP	6	15	22
5	74	m	180	3	5	CBP	7	18	4
6	58	f	168	7	6	CBP	19	22	21
7	65	m	48	6	5	CBP	4	11	12
8	65	f	132	3	3	CBP	6	5	24
9	76	f	24	5	5	CBP	4	9	20
10	33	f	36	6	7	CBP	9	19	16
11	45	f	12	8	7	CBP	5	20	8
12	51	f	24	5	6	CBP	11	22	19
13	73	f	108	6	8	CBP	11	21	26
14	41	f	120	5	6	CBP	13	14	13
15	55	f	252	9	9	CBP	24	24	20
16	73	m	300	5	4	CBP	4	10	5
17	46	m	360	6	7	CBP	16	10	5
18	50	m	60	7	7	CBP	0	5	17
19	59	f	24	4	6	CBP	12	31	23
20	62	m	12	5.5	6	CBP	10	26	22
21	54	m	84	5	7	CBP	16	18	17
22	39	f	144	4	2	CBP	0	12	22
23	66	m	48	4	4	CBP	8	19	10
24	57	m	300	5	6	CBP	22	12	17
25	52	m	300	4	3	CBP	11	22	13
26	47	f	180	4	3.5	CBP	26	19	15
27	24	f	96	7.5	7.5	CBP	5	13	20
28	59	f	180	3	5	CBP	6	4	10
29	82	m	60	5	5	CBP	14	21	8
30	54	m	120	6.5	6	CBP	12	17	22
31	62	f	36	3	4.5	CBP	3	22	11
32	73	m	480	8	8	CBP	4	11	10
33	48	m	64	0.5	4	CBP	24.45	24	22
34	55	f	240	5	6	CBP	8.55	31	11
35	59	f	60	3	4	PNP	13.5	11	15
36	48	f	108	3	4	PHN	15.4	13	28
37	73	f	24	5	5	CBP	13.5	5	11
38	57	m	84	8	7.5	PNP	22.35	15	33
39	57	f	96	6	7	CBP	3.4	20	15
40	77	f	36	5	7.8	PNP	4	10	11
41	77	f	480	3.5	3.5	CBP	8.6	9	19
42	53	f	24	4	5	CBP	16.3	12	24
43	80	m	48	4	4	PHN	11.4	4	18
44	77	f	192	4	6	CWP	12.8	0	23
45	57	f	72	5	6	CWP	5.7	42	17
46	67	f	21	6	8	NP	3.4	8	17
47	77	f	324	6	6	CWP	3.4	16	24
48	61	f	36	4.5	6	NP	3.4	7	21.5
49	65	f	23	8	8	CWP	4	7.5	25

ID	Age	Sex	Pain duration	Curr. pain	Avg. Pain	Pain	MQS	BDI	PDQ
50	65	f	180	5	4	CWP	0	12	22
51	56	f	213	4	7	CWP	8	13	23
52	57	m	264	3	4	JP	13.25	10	11
53	41	f	24	4	5	NP	25.5	12	24
54	69	f	72	8	5	CBP	0	19	13
55	56	f	108	8	8	PNP	17.2	10	25
56	72	f	120	7	8	CWP	15.4	16	20
57	57	m	96	5	7	PNP	10.9	11	28
58	82	f	36	2	5	CBP	4.6	n.a.	10
59	70	f	420	4	6	CWP	14.8	28	22
60	70	f	72	4	6	PHN	10.3	11	22
61	54	f	24	7	5	PHN	5.8	10	10
62	69	f	48	6	5	PHN	8.4	6	16
63	66	f	84	2	3	JP	6	4	13
64	52	f	204	6	6	CWP	10.2	16	21
65	77	f	72	8	8	JP	4.6	n.a.	19
66	42	m	252	7	9	CBP	17.35	33	22
67	51	f	31	6	5	JP	9.1	15	7
68	55	m	7	7	7	JP	6.9	1	13
69	68	f	24	1	4	NP	3.8	0	23
70	71	m	324	4	5	CBP	10.8	5	6
71	24	f	108	6	6	CWP	8	31	21
72	71	m	36	6	6	CBP	5.8	9	14
73	68	f	204	3	4	JP	8.8	7	15
74	86	f	120	3	3	CBP	2	5	6
75	68	f	120	4	5	NP	7.8	5	28
76	45	m	48	1	2	CBP	3.8	10	9
77	18	f	16	4	6	PHN	0	14	20
78	80	f	25	8	7	PHN	23.1	15	20
79	60	m	60	n.a.	n.a.	PNP	0	n.a.	n.a.
80	60	f	54	3.5	5.5	CBP	13.5	22	18
81	57	m	17	6.5	6.5	CBP	24.3	25	24
82	45	m	n.a.	7.3	n.a.	CWP	0	17	n.a.
83	24	f	n.a.	3.2	n.a.	CWP	0	17	n.a.
84	49	m	n.a.	7.3	n.a.	CWP	0	39	n.a.
85	47	f	n.a.	2.4	n.a.	CWP	0	21	n.a.
86	53	f	n.a.	7.5	n.a.	CWP	0	22	n.a.
87	41	f	n.a.	6.2	n.a.	CWP	0	29	n.a.
88	46	m	n.a.	7.4	n.a.	CWP	0	20	n.a.
89	56	f	n.a.	1.8	n.a.	CWP	0	22	n.a.
90	55	f	n.a.	7.8	n.a.	CWP	0	30	n.a.
91	60	f	n.a.	6.2	n.a.	CWP	0	14	n.a.
92	55	f	n.a.	8.6	n.a.	CWP	0	25	n.a.
93	48	f	n.a.	2.9	n.a.	CWP	0	27	n.a.
94	59	m	n.a.	6.8	n.a.	CWP	0	13	n.a.
95	60	f	n.a.	5	n.a.	CWP	0	17	n.a.
96	58	f	n.a.	4.5	n.a.	CWP	0	12	n.a.
97	71	f	n.a.	8.4	n.a.	CWP	0	36	n.a.
98	42	m	n.a.	3.7	n.a.	CWP	0	12	n.a.
99	38	f	n.a.	6.5	n.a.	CWP	0	10	n.a.
100	65	f	n.a.	8.8	n.a.	CWP	0	18	n.a.
101	60	f	n.a.	6	n.a.	CWP	0	21	n.a.

ID, patient identification number; ys, years; Curr. pain, currently experienced pain; Avg. pain, average pain in the last 4 weeks; VAS, visual analog scale: 0 = no pain, 10 = worst imaginable pain; MQS, medication quantification scale; BDI, Beck Depression Inventory II, score $\geq$ 18 = clinically relevant depression; PDQ, painDETECT, score $\geq$ 19 = neuropathic pain component probable; m, male; f, female; CBP, chronic back pain; PNP, poly-neuropathic pain; NP, neuropathic pain, PHN, post-herpetic neuralgia; CWP, chronic widespread pain; JP, joint pain; n.a., not available because the respective questionnaire was not completed.

2.2 Recordings

Brain activity was recorded using EEG. Recordings were performed during the resting-state, i.e. participants were asked to stay in a relaxed and wakeful state, without any particular task. EEG data were recorded with eyes closed and eyes open for 5 minutes each. As the eyes closed condition showed better data quality and less muscle artifacts, analyses were focused on this condition. EEG data were recorded using 64 electrodes consisting of all 10-20 system electrodes and the additional electrodes Fpz, CPz, POz, Oz, Iz, AF3/4, F5/6, FC1/2/3/4/5/6, FT7/8/9/10, C1/2/5/6, CP1/2/3/4/5/6, TP7/8/9/10, P5/6 and PO1/2/9/10 plus 2 electrodes below the outer canthus of each eye (Easycap, Herrsching, Germany) and BrainAmp MR plus amplifiers (Brain Products, Munich, Germany). All EEG electrodes were referenced to FCz and grounded at AFz. Simultaneously, muscle activity was recorded with 2 bipolar surface electromyography (EMG) electrode montages placed on the right masseter and neck (semispinalis capitis and splenius capitis) muscles and a BrainAmp ExG MR amplifier (Brain Products, Munich, Germany). The EMG ground electrode was placed at vertebra C2. All data were sampled at 1000 Hz (0.1 μV resolution) and band-pass filtered between 0.016 Hz and 250 Hz. Impedances were kept below 20 kΩ. Prior to the EEG recordings, patients completed the following questionnaires to assess pain characteristics and comorbidities: short-form McGill Pain Questionnaire (SF-MPQ) (Melzack, 1987), Pain Disability Index (PDI) (Dillmann et al., 1994), painDETECT (PDQ) (Freynhagen et al., 2006), Beck Depression Inventory II (BDI-II) (Beck et al., 1996), State-Trait-Anxiety Inventory (STAI) (Spielberger et al., 1983) and the Veteran's RAND 12-Item Health Survey (VR-12) (Selim et al., 2009).

2.3 Preprocessing

Preprocessing was performed using the BrainVision Analyzer software (Brain Products, Munich, Germany). Data were downsampled to 250 Hz to improve computation speed. For artifact identification, a high-pass filter of 1 Hz and a 50 Hz notch filter for line noise removal were applied to the EEG data. Independent component analysis was performed (Jung et al., 2000) and components representing eye movements and muscle artifacts were identified based on time courses and topographies. Furthermore, time intervals of 400 ms around data points with signal jumps exceeding $\pm$ 100 μV were marked for rejection. Lastly, all data were visually inspected and remaining bad segments marked. Subsequently, independent components representing artifacts were subtracted from the raw, unfiltered EEG data and EEG data were re-referenced to the average reference. The reference electrode FCz was added to the signal array. Next, data were exported from the BrainVision Analyzer and further analyzed in Matlab (Mathworks, Natick, MA, USA) with the FieldTrip (Oostenveld et al., 2011) and Brain Connectivity Toolbox (Rubinov and Sporns,

2010), along with custom-written code. Data were segmented into 2-second epochs with 1 second overlap. A 2-second epoch length was chosen to balance the stationarity of the signals and the number of samples for lower frequencies (Chu et al., 2012; van Diessen et al., 2015). All analyses are based on these epochs and the following 4 frequency bands: theta (4 – 8 Hz), alpha (8 – 13 Hz), beta (14 – 30 Hz) and gamma (60 – 100 Hz). We observed strong non-stationary line noise around 45 – 55 Hz and therefore excluded the "low gamma" band from frequency band specific analyses.

For the following analyses, we define two categories. First, local, i.e. spatially specific, analyses were performed in which a single value is obtained for every electrode, voxel or brain region. These analyses include the comparison of power topographies on electrode level and connectivity and local network measures topographies (degree, CC) on source level. Second, global, i.e. spatially holistic, analyses were performed. These analyses include all analyses which average across all electrodes, voxels or brain regions, i.e. the peak frequency, the power spectrum and all global network measures (gCC, gEff, S, Q, kd). In all global analyses, each participant is represented by a single scalar value per measure.

2.4 Brain Activity (Power) Analysis

Frequency-specific global power was computed on electrode level for all epochs using a Fast Fourier Transformation (FFT) with Slepian multitapers (Thomson, 1982) and a frequency smoothing of 1 Hz and then averaged across epochs and electrodes. Power was first computed for the complete power spectrum, i.e. 1 – 100 Hz, with a frequency resolution of 0.5 Hz. To remove line noise, a band-stop filter of 45 – 55 Hz was applied before computing power. The individual dominant peak frequency was determined on the average of the epochs as the highest local maximum (larger than its two neighboring samples) of the amplitude in the frequency range of 6 – 14 Hz (Bazanova and Vernon, 2014). Another method is to define the center of gravity of the power spectrum as the peak frequency (Klimesch, 1999; Bazanova and Vernon, 2014). We also computed the dominant peak frequency with both methods using longer time windows of 5 seconds to control for the length of time windows. We also re-computed this analysis by computing the peak frequency on each single epoch and then averaging the peaks (Furman et al., 2017). To compare the spatial distribution of local brain activity between patients and healthy controls, power was averaged within each frequency band before comparing groups with cluster-based permutation tests. Relative power was calculated by normalizing every power value (both local and global power) by the respective participant's total power. Total power was calculated by summing all power values across frequencies 1 to 100 Hz and across all electrodes.

2.5 Source Analysis

We used linearly constrained minimum variance (LCMV) beamforming (van Veen et al., 1997) to project the band-pass filtered data for each frequency band and participant from electrode space into source space. Spatial filters were computed based on the covariance matrices of the band-pass filtered data for each frequency band and a lead field matrix. A three-dimensional grid with a 1 cm resolution covering the brain was defined, resulting in a total of 2020 voxels in the brain. The lead field was constructed for each voxel using a realistically shaped 3-shell boundary-element volume conduction model based on the template Montreal Neurological Institute (MNI) brain. We used a regularization parameter of 5 percent of the covariance matrix and chose the dipole orientation of most variance using singular value decomposition. Finally, the preprocessed and bandpass-filtered EEG data were projected through the spatial filter to extract the amplitude time series of neuronal activity of each frequency band at each voxel.

2.6 Connectivity Analysis

Functional connectivity was investigated using 3 different connectivity measures: the phase locking value (PLV) (Lachaux et al., 1999), the debiased weighted phase lag index (dwPLI) (Vinck et al., 2011) and the orthogonalized amplitude envelope correlation (AEC) (Hipp et al., 2012). Both PLV and dwPLI are based on the phase of the signals, whereas the AEC is based on the amplitude. Thus, we assessed the complementary information provided by phase and amplitude-based connectivity measures (Engel et al., 2013). Amplitude-based connectivity is more closely related to structural connectivity (Vincent et al., 2007; Wang et al., 2013), putatively regulating activation of whole brain regions and being implicated in diseases with dominant structural alterations (Engel et al., 2013). Phase-based connectivity seems more detached from structure and is strongly affected by contextual factors (Singer, 1999; Siegel et al., 2012). The PLV is well-established, highly sensitive and captures both zero-phase lag and non-zero-phase lag connectivity. The dwPLI captures non-zero phase lag connectivity only. The dwPLI is therefore not susceptible to volume conduction at the cost of reduced sensitivity because real synchrony at zero phase lag is also discarded. All our connectivity analyses are based on contrasts between two groups and are therefore less susceptible to effects of volume conduction. Additionally, if no group differences in amplitude are found, the probability of connectivity differences being driven by volume conduction is further reduced.

For the connectivity analyses, the connectivity between every pair of voxels was computed, resulting in a 2020 x 2020 matrix, with a single value representing the strength of connection between two voxels over the complete recording time. All 3 connectivity measures are undirected.

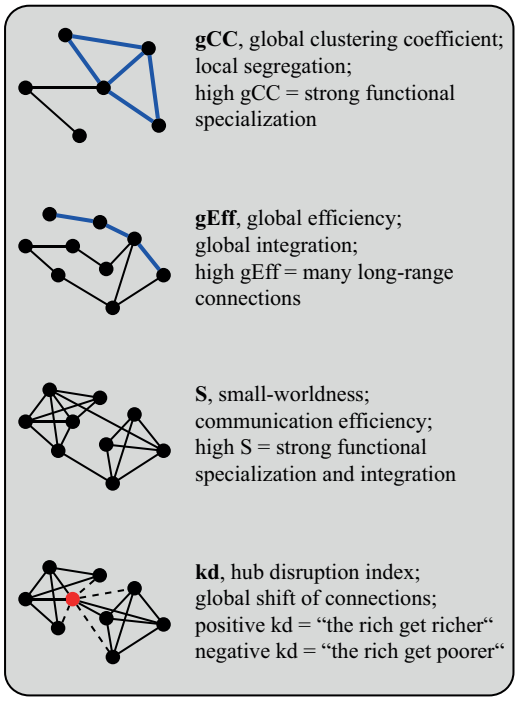

Figure 10: Global graph-theoretical measures.

A summary of the global graph measures relevant for this study. The global clustering coefficient (gCC) quantifies the number of connections that exist between the nearest neighbours of a node as a proportion of the maximum number of possible connections (Watts and Strogatz, 1998). Random networks have low average clustering whereas complex networks have high clustering, associated with high local efficiency of information transfer and robustness (Bullmore and Sporns, 2009). The path length is the number of edges that must be traversed to reach another node from a starting node (Watts and Strogatz, 1998). The global efficiency (gEff) is inversely related to the average shortest path length between all possible pairs of nodes, so high global efficiency (= short path lengths on average) is thought to reflect high connectome integration (Achard and Bullmore, 2007). Small-worldness (S) combines the clustering coefficient and the global efficiency, resulting in a compound measure (Humphries and Gurney, 2008). A high small-worldness supports functional segregation and integration, as well as information propagation (Bassett and Bullmore, 2006). The hub disruption index (k_d) is a complex measure which compares the degree of all nodes to those of a control group (Achard et al., 2012). Positive values indicate that strongly connected nodes increase and weakly connected nodes decrease their number of connections ("the rich get richer and the poor get poorer"). Conversely, negative values indicate that strongly connected nodes decrease and weakly connected nodes increase their number of connections ("the rich get poorer and the poor get richer"), which means a shift of the network towards a random network with less internal structure (Achard et al., 2012; Mansour et al., 2016).

2.7 Graph-theoretical Network Analysis

Graph theory is a branch of mathematics treating systems of interacting elements. The two elementary components in graph theory are nodes and edges connecting the nodes. Graphs are a useful tool to analyze complex networks, offering a flexible and established mathematical framework. We refer to Sporns (2012) as an excellent introduction to this topic in the context of brain networks. Fundamentally, graphs are an abstract construct reflecting the underlying systems. They enable quantitative comparisons across different brain networks because these networks share certain key organizational principles even if they differ on a microscopic level (Bullmore and Sporns, 2009). Further, graph theory can effectively reduce dimensionality of data, reducing the amount of statistical tests necessary to compare between groups. Graph theory has recently become more feasible for neuroimaging studies (Sporns, 2011) because of the substantial increase in computational power, a necessity for the large amount of data generated in most neuroimaging recordings. This has led to a growing body of research associating neurological diseases with abnormal structural and functional brain network measures, e.g. in Alzheimer's disease (Stam, 2014).

By applying graph-theoretical methods to our data, we reduced the high-dimensional EEG data to a few network measures, characterizing the organization of the whole

brain network. We defined the nodes as voxels and the edges as thresholded functional connectivity between voxels. To reduce the complexity of the analysis, the adjacency matrix (the matrix defining all edges between the nodes) was thresholded to the 10 (5, 20, see Figure 20 and Figure 21) percent of strongest connections and binarized, resulting in an unweighted and undirected graph. We used graph measures that characterize either a single node (local analyses) or the complete network (global analyses).

We investigated two local network measures: the degree and the local clustering coefficient. The degree is the number of connections to other nodes. The local clustering coefficient (CC) is the fraction of the node's neighbors that are also neighbors of each other (Rubinov and Sporns, 2010). Thus, both local measures depict the importance of a node. Four global network measures were included in the analysis (see Figure 10): the global clustering coefficient (gCC), global efficiency (gEff), small-worldness (S) and hub disruption index (kd) (Achard et al., 2012). The global clustering coefficient is the average of the local clustering coefficient of all nodes, resulting in a measure of local segregation (Rubinov and Sporns, 2010; Fornito et al., 2016). The gEff is the inverse of the average shortest path length. It measures the strength of "long-range" connections or the global integration (Rubinov and Sporns, 2010; Fornito et al., 2016). S describes the ratio of clustering coefficient and global efficiency and compares it to random networks. Lastly, the hub disruption index is a differential measure and compares the degree of a node to its average degree in a control cohort. It shows potential shifts of connections, which manifest on a global scale (Achard et al., 2012; Mansour et al., 2016).

2.8 Correlation Analysis

Pearson's r was computed between clinical parameters and brain measures which had been found to show a significant correlation with clinical parameters in previous studies (Sarnthein et al., 2006; Stern et al., 2006; Schmidt et al., 2012; de Vries et al., 2013; Gonzalez-Roldan et al., 2016; Mansour et al., 2016; Kuo et al., 2017; Vanneste et al., 2017; Choe et al., 2018; Fallon et al., 2018). Additionally, the brain measures that were found to significantly differ between chronic pain patients and healthy controls in this study were tested for correlation with clinical parameters. The global peak frequency, mean global power in the four frequency bands, hub disruption index and the mean theta and gamma PLV connectivity, the PLV global efficiency in the gamma band, and the dwPLI hub disruption index in the gamma band, were correlated with the following clinical parameters: current pain intensity, average pain intensity in the last four weeks quantified by a visual analog scale, pain duration, pain disability quantified by the PDI, mental and physical quality of life quantified by the VR-12, depression quantified by the BDI-II, and medication as quantified by the medication quantification scale (MQS)(Harden et al., 2005).

2.9 Machine Learning Analysis

2.9.1 Fundamentals of machine learning

All the above analyses were univariate comparisons between the two groups, investigating one specific feature of the EEG sequentially. All these comparisons of different features were done independently of one another, e.g. the comparison of the peak frequency was tested independently from the global power spectrum. As discussed in 1.1.4 and 1.1.5, both experimental and chronic pain are most likely represented by complex patterns of brain activity spanning the temporal, spectral and spatial dimensions of EEG activity. A tool to investigate patterns of data that has has recently gained large public and scientific interest because of its outstanding performance, especially in the fields of computer vision and language processing, is machine learning (Jordan and Mitchell, 2015). It is a generic term for a family of computer algorithms which learn a set of rules or representations without explicit programming (Bishop, 2006). In general, all kinds of machine learning scale extremely well with the amount of data available up to a certain point, i.e. the more data, the better the performance (Alpaydin, 2014). The focus in this work will be on a specific rule-based classifier, a Support Vector Machine (SVM) (Cortes and Vapnik, 1995).

The basic principle of an SVM is to fit a so-called hyperplane to achieve the best discrimination between two classes; this is schematically depicted in Figure 11. In the simple case of e.g. two-dimensional data, a hyperplane would simply be a line, while a hyperplane in three-dimensional data would be an actual plane, and generally in n-dimensional data a hyperplane would be an (n-1)-dimensional plane. New data points are simply classified as belonging to one class or the other depending on which side of the hyperplane they are located. As one of the most commonly used, simplest and most easily intrepretable machine learning algorithms, we chose an SVM as a first approach to differentiate between chronic pain patients and healthy controls via machine learning.

2.9.2 Support vector machines

The machine learning analysis was carried out using the Statistics and Machine Learning Toolbox in Matlab as well as custom-written scripts. We implemented an SVM with a linear kernel, which was trained on all available features. The features were the peak frequency (1 feature per participant), global power spectrum (199 features per participant, 1 feature for each frequency step), local power (4 x 65 features per participant, 4 frequency bands, 65 electrodes), local strength of connectivity (3 x 4 x 2020 features per participant, 2020 voxels in 4 frequency bands and 3 connectivity measures), local degree (3 x 4 x 2020 features per participant, 2020 voxels in 4 frequency bands and 3 connectivity measures), local clustering

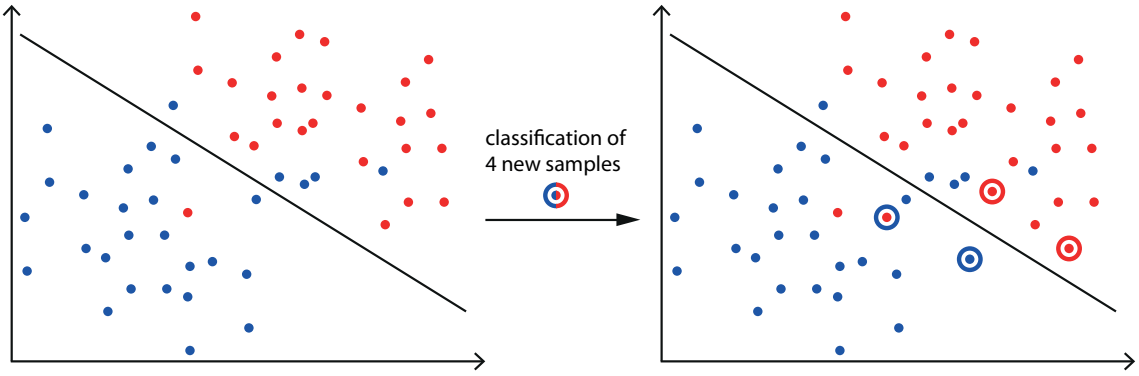

Figure 11: Basic principle of an SVM.

A schematic visualization of how a classification with an SVM works. A simple example of two-dimensional data with two groups (red and blue) is shown. The discriminatory function in this case is the black line, trained with the training data on the left. New data is classified by looking at which side of the line the samples are located. Here, the inner circle represents the ground truth, i.e. which group the data sample really belongs to, while the outer circle represents the classification result. In this example, 3 out of 4 new samples are classified correctly, which would result in a classification accuracy of 75 percent.

coefficient (3 x 4 x 2020 features per participant, 2020 voxels in 4 frequency bands and 3 connectivity measures), and the global graph measures (3 x 4 x 4 features per participant, 4 global graph measures in 4 frequency bands and 3 connectivity measures). This resulted in an SVM containing 73228 features per participant. To avoid overfitting, we implemented a so-called sequential forward feature selection. This algorithm consists of incrementally adding single features to the SVM and evaluating the performance. When performance is increased, the feature is kept and another feature is added. If performance of the SVM is not improved, the feature is discarded and a different feature is added. This process is repeated until no additional feature improves performance. The performance of the SVM was evaluated using a 10-fold cross-validation. First, the dataset was randomly split into 10 folds. 9/10 folds were used to train the classifier, after which the remaining 1/10 were classified, resulting in a certain classification accuracy. This procedure was then repeated, cycling through all folds, yielding a mean accuracy over the 10 folds. As our groups were unbalanced regarding participant numbers, we randomly picked 84 datasets from the cohort of chronic pain patients for the classification procedure, repeating this 1000 times. To conclude whether this result truly exceeds chance level, we repeated the whole procedure with the same data, but the labels of chronic pain patients and healthy controls were randomly shuffled. The two resulting distributions were then statistically compared using a non-parametric permutation test. The sensitivity is defined as the rate of true positives, i.e. correctly classified patients, divided by the number of total patient classifications. The specificity is defined as the rate of true negatives, i.e. correctly classified healthy controls, divided by the number of total healthy classifications. Apart from the overall performance of the SVM, we also investigated which features contained the highest predictive

value, i.e. which features were most consistently picked by the SVMs by looking at the number of times a certain feature was included in the SVM by automatic feature selection.

2.10 Statistical Analysis

Statistical analysis was carried out using FieldTrip and custom-written Matlab scripts. The significance level for all statistical tests was set to 0.05 two-tailed. We used cluster-based permutation tests with a cluster-threshold of 0.05 to compare patients to healthy controls for all local analyses and the global power spectrum analysis (Maris and Oostenveld, 2007). We report maximal and minimal T-values ($t_{max/min}$) for all cluster-based permutation tests to show potential trends. The other global measures were compared using non-parametric permutation tests, permuting between the patient and healthy control group. The underlying statistical test for all permutation tests was an unpaired T-test. To account for multiple comparisons within a specific measure, we corrected all p-values of tests that were performed on all 4 frequency bands using the Holm-Bonferroni method (Holm, 1979). To test whether the accuracy of the SVMs was above random chance level, we computed a non-parametric permutation test on the accuracy distribution of the SVM trained on the real data against the accuracy distribution of the SVM trained on the randomly labeled data. Pearson's r was calculated to find correlations between brain measures and clinical parameters and tested for statistical significance against the null hypothesis of no correlation. Resulting p-values were again corrected for multiple comparisons across the four frequency bands using the Holm-Bonferroni method, if applicable.

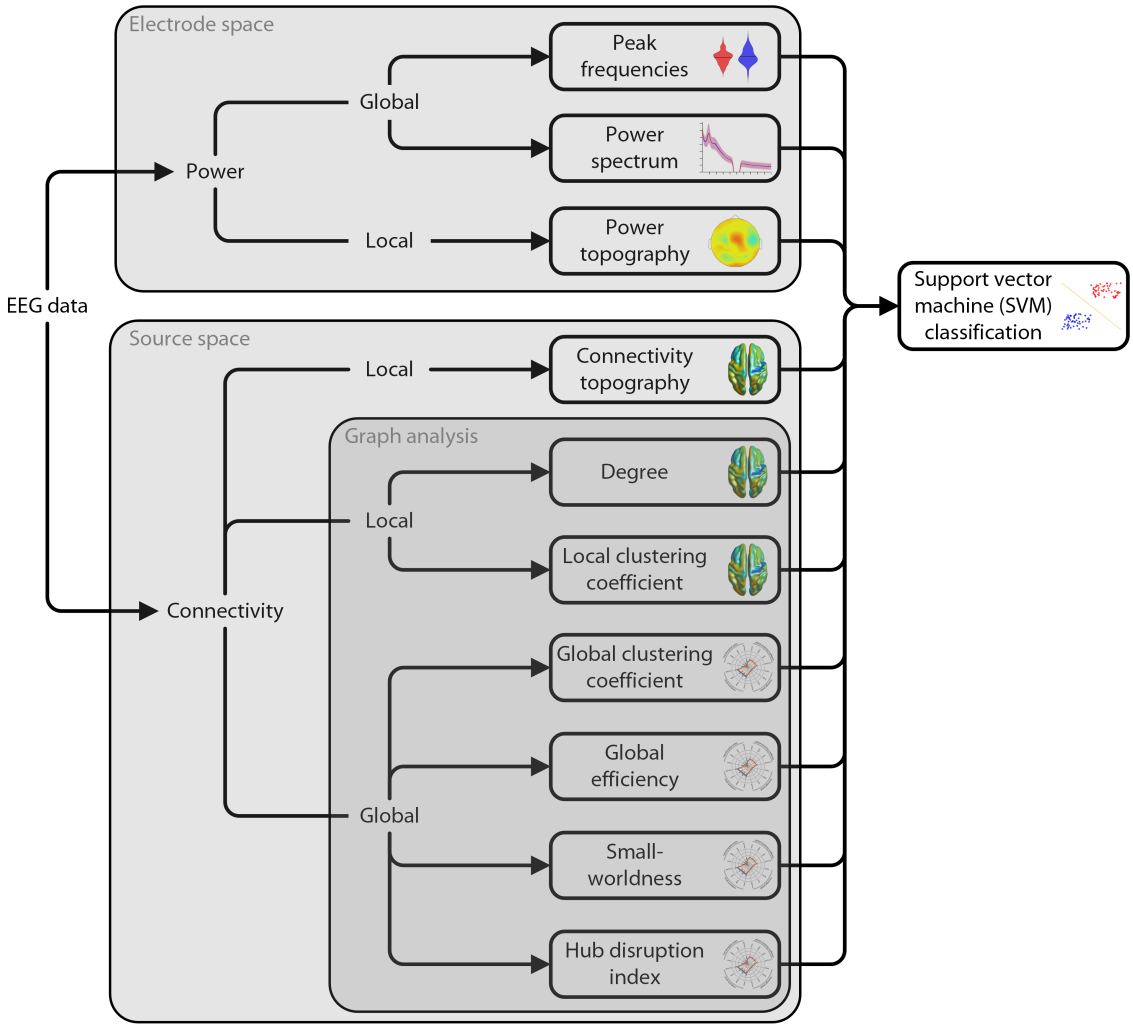

Figure 12: Analysis pipeline.

EEG data were analyzed with regard to power and connectivity, which quantify neural activity and neural communication, respectively. Power analyses were performed in electrode space. Analyses of functional connectivity were performed in source space. Connectivity analyses comprised phase-based (PLV and dwPLI) and amplitude-based (AEC) connectivity measures. Graph theoretical network analysis was applied to further characterize functional connectivity. All measures were compared between chronic pain patients and healthy controls. In addition, a purely data-driven machine learning approach was adopted, using an SVM. The SVM was trained on all power and connectivity measures to distinguish between chronic pain patients and healthy controls.

3 Results

We collected resting-state EEG data from 101 patients suffering from chronic pain and 84 age and gender-matched healthy, pain-free controls. Demographic and clinical data of participants are shown in Table 2 and Table 3, respectively. In order to define abnormalities of brain function in chronic pain regardless of subtype, patients suffering from various types of chronic pain were included. Figure 12 summarizes the analyses of the EEG data. They included measures of the magnitude of brain activity (power) and connectivity between brain regions in electrode and source space, respectively. Power and connectivity analyses comprised local and global analyses. We define local analyses as spatially specific analyses in which a single value was obtained for each electrode, voxel or brain region. These analyses included topographies of power, connectivity and local network measures. In contrast, we define global analyses as spatially holistic analyses in which a single value was obtained for each participant. These analyses summarized the data of different electrodes, voxels or brain regions, i.e. the peak frequency, the power spectrum and global network measures. All analyses were based on 2-second epochs of resting-state data unless stated otherwise, to balance robustness, frequency resolution and non-stationarity of the data.

3.1 Global Measures of Brain Activity

First, we investigated whether chronic pain was associated with global changes of brain activity on electrode level. We determined the peak frequency of EEG activity in chronic pain patients and healthy controls by averaging the power spectra across all epochs and electrodes and determining the maximal power in the frequency range of 6 to 14 Hz (Bazanova and Vernon, 2014). Peak frequency was 9.8 ± 1.2 Hz (mean ± standard deviation) in chronic pain patients and 10.0 ± 1.4 Hz in healthy controls and did not differ significantly between groups (non-parametric permutation test, $p = 0.20$, Figure 13A). Other common approaches to determine the peak frequency, by computing the center of gravity, analyzing longer time windows (5 seconds) for increased spectral resolution, or computing the peak frequency on individual epochs and then averaging, did not show a difference between groups either (Figure 14).

Next, we examined whether chronic pain was associated with global changes of oscillatory brain activity at any frequency between 1 and 100 Hz. To this end, we compared the global power spectrum of EEG activity averaged across all electrodes

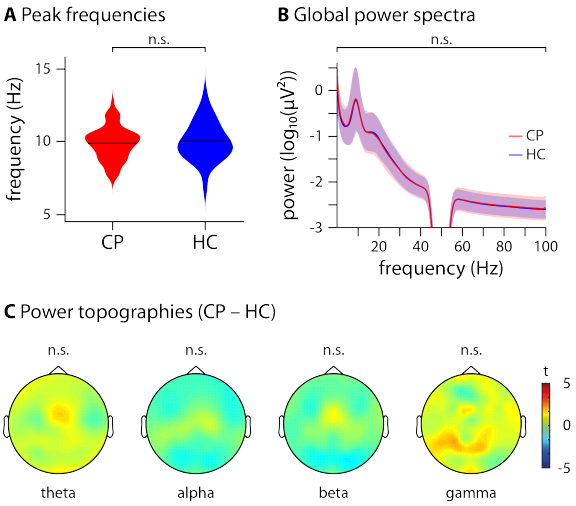

Figure 13: Global and local measures of brain activity - absolute power.

(**A**) Violin plot of the dominant peak frequencies computed on the average across all electrodes of chronic pain patients (CP, red) and healthy controls (HC, blue). A non-parametric permutation test showed no significant difference ($p = 0.20$) between the two groups. (**B**) Global power spectra of CP (red) and HC (blue), averaged across all electrodes and shown for the frequencies 1 – 100 Hz, with a bandstop filter at 45 – 55 Hz to remove line noise. A cluster-based permutation test clustered across frequencies did not show any significant differences ($t_{max/min} = 1.7/-1.5$). (**C**) Scalp topographies of power differences between CP and HC at theta, alpha, beta and gamma frequencies, averaged across frequencies in each band. The colormap shows the t-values of a cluster-based permutation test. No significant clusters were found in any frequency band (theta $t_{max/min} = 1.5/-0.6$, alpha $t_{max/min} = 0.62/-1.2$, beta $t_{max/min} = 1.0/-1.4$, gamma $t_{max/min} = 2.1/-0.7$).

between chronic pain patients and healthy controls. The results did not reveal any significant difference between the two groups at any frequency (cluster-based permutation statistics clustered across frequencies, $t_{max/min} = 1.7/-1.5$; Figure 13B). When controlling for inter-subject differences in overall power by calculating power relative to the total power across all electrodes and frequencies for each participant, the results did not show a significant difference between patients and controls either ($t_{max/min} = 1.4/-1.7$; Figure 15A).

Thus, we did not observe global changes of the peak frequency or the power spectrum of oscillatory brain activity in chronic pain patients.

3.2 Local Measures of Brain Activity

We further assessed whether chronic pain was associated with local changes of oscillatory brain activity. We therefore calculated topographical maps of brain activity for theta (4 – 8 Hz), alpha (8 – 13 Hz), beta (14 – 30 Hz) and gamma (60 – 100 Hz) frequency bands. Group comparisons of the topographical maps did not show significant differences between patients and controls in any frequency band (cluster-based permutation statistics clustered across electrodes, $t_{max/min} = 2.0/-1.4$, Figure 13C). When controlling for inter-subject differences in overall power by calculating relative power, the results did not show a significant difference between patients and controls either ($t_{max/min} = 2.5/-3.2$; Figure 15B).

Thus, our findings did not show local changes of oscillatory brain activity in chronic pain patients in any frequency band. Taken together, as neither global nor local brain activity differed between chronic pain patients and healthy controls, any potential connectivity effects are unlikely to be driven by volume conduction.

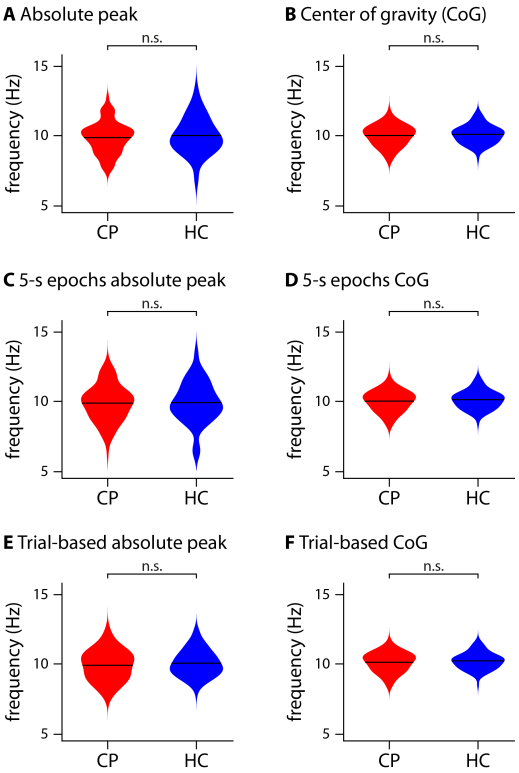

Figure 14: Global measures of brain activity - alternative peak frequency analyses.

(**A**)Peak frequency analysis as reported in Figure 13A. (**B**) Peak frequency analysis was repeated with the center of gravity method, which defines the center of gravity of the power spectrum as the peak frequency. The comparison of chronic pain patients (CP, red) and healthy controls (HC, blue) with a non-parametric permutation test did not show a significant difference ($p = 0.16$). (**C**) Peak frequency analysis as described in Figure 13A was repeated with 5 second epochs. No significant difference between patients and healthy controls was found ($p = 0.43$). (**D**) Peak frequency analysis using the center of gravity method based on 5 second epochs. No significant difference between chronic pain patients and healthy controls was found ($p = 0.14$). (**E**) The peak frequency of each participant was calculated by determining the peak frequency of each single epoch and then averaging across epochs and electrodes. No significant difference between patients and healthy controls was found ($p = 0.15$). (**F**) The peak frequency of each participant was calculated by determining the peak frequency of each single epoch using the center of gravity method and then averaging across epochs and electrodes. No significant difference between patients and healthy controls was found ($p = 0.15$).

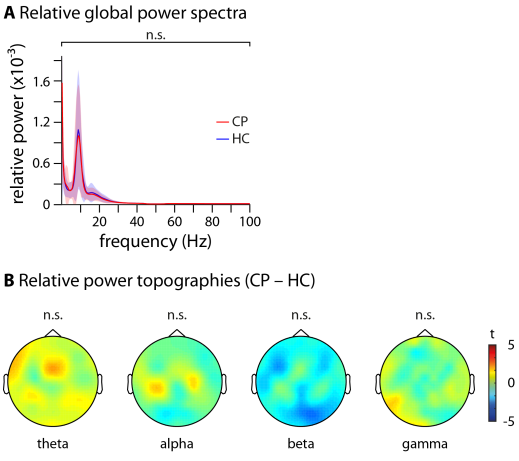

Figure 15: Global and local measures of brain activity - relative power.

(**A**) Same as Figure 13B, but power values were normalized for each participant by the participant's total power, i.e. the power summed across all electrodes and frequencies (1 to 100 Hz). A cluster-based permutation test clustering across frequencies did not show a significant difference between chronic pain patients (CP, red) and healthy controls (HC, blue) ($t_{max/min} = 1.4/-1.7$). (**B**) Same as Figure 13C, but all power values were normalized for each participant by the participant's total power. The colormap shows the t-values of a cluster-based permutation test. No significant cluster was found in any frequency band (theta $t_{max/min} = 2.5/-1.7$, alpha $t_{max/min} = 2.3/-2.3$, beta $t_{max/min} = 1.2/-3.2$, gamma $t_{max/min} = 1.2/-2.3$).

3.3 Local Measures of Functional Connectivity

Next, we explored whether chronic pain was associated with changes of functional connectivity, a measure of neural communication. To reduce potential confounds by field spread and volume conduction effects (Schoffelen and Gross, 2009), we performed all connectivity analyses in source space using 2020 voxels with a size of 1 x 1 x 1 cm^3. We then computed the connectivity between all pairs of voxels, resulting in a connectivity matrix of dimension 2020 x 2020. Connectivity analyses of EEG data can be performed using phase-based and amplitude-based approaches which capture different and complementary neural communication processes (Engel et al., 2013). Amplitude-based connectivity is more closely related to structural connectivity and putatively regulates activation of brain regions. Phase-based connectivity seems more detached from structure and is more strongly affected by contextual factors. We therefore performed both phase-based and amplitude-based connectivity analyses by calculating the PLV and the AEC, respectively. As a more conservative measure which also discards zero phase-lag connectivity, we also analyzed connectivity using the dwPLI, which will be reported further below.

We first investigated whether chronic pain was associated with local changes of functional connectivity in any brain region or any frequency band. To this end, we calculated the connectivity strength for each voxel and frequency band. Connectivity strength was defined as the average connectivity of a specific voxel to all other voxels of the brain, which yields one connectivity strength value for each voxel. This allows for visualizing connectivity strength in a topographical map and applying the same statistical approaches used for the analysis of local brain activity. Analysis of phase-based connectivity (Figure 16A) showed that chronic pain patients' connectivity strength in the theta band was significantly increased (cluster-based permutation test, p(corrected/uncorrected) = 0.045/0.011, Cohen's d = 0.40) in comparison to the control group. The strongest contrast was found in the supplementary motor area (MNI = [-10, 10, 70]). Moreover, we also found that patients showed a significantly increased connectivity strength in the gamma band (cluster-based permutation test, p(corrected/uncorrected) = 0.0072/0.0018, Cohen's d = 0.59), which was maximal in the anterior prefrontal cortex (MNI = [-40, 40, 30]). No significant clusters were found in the alpha and beta bands (alpha: p_{min}(corrected/uncorrected) = 1/0.61, t_{max} = 2.8; beta: p_{min}(corrected/uncorrected) = 0.71/0.18, t_{max} = 3.5). Analysis of amplitude-based connectivity did not show any significant differences in connectivity strength between chronic pain patients and healthy controls in any brain region or any frequency band. (Figure 16B, $t_{max/min}$ = 0.4/-1.2).

To further assess connectivity patterns of chronic pain patients, we performed graph theory-based network analysis. Graph theory conceptualizes a network as a collection of nodes and their connections, termed edges. Here, nodes were defined as voxels and edges as thresholded functional connectivity between voxels. To simplify the subsequent analyses, edges were thresholded to the 10 percent

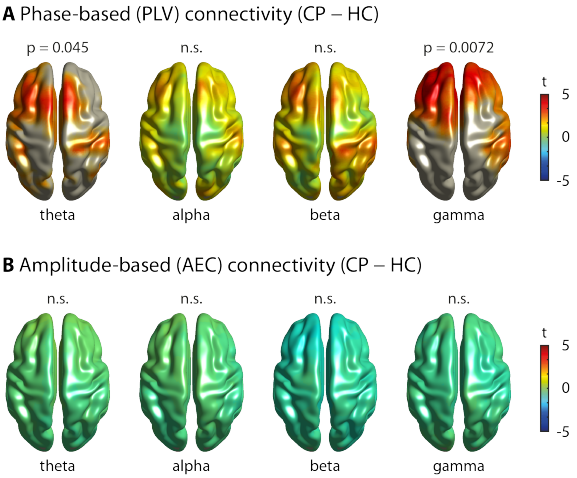

Figure 16: Local measures of functional connectivity. Brain topographies of the comparison of connectivity strength between chronic pain patients (CP) and healthy controls (HC) in the theta, alpha, beta and gamma band frequencies, averaged across frequencies in each band, are shown. Connectivity strength was calculated as the average connectivity of one voxel to all other voxels of the brain. The colormaps show the t-values. Significant results are masked, i.e. all voxels but the ones belonging to a significant cluster are greyed out. When no significant clusters are found, nothing is greyed out to show potential trends. (**A**) PLV. A significant increase of chronic pain patients' connectivity strength was observed in the theta band (p(corrected/uncorrected) = 0.045/0.011, t_{max} = 3.8, Cohen's d = 0.40) and the gamma band (p(corrected/uncorrected) = 0.0072/0.0018, t_{max} = 5.1, Cohen's d = 0.59). (**B**) AEC. No significant differences were found in any frequency band (theta $t_{max/min}$ = 0.4/-0.6, alpha $t_{max/min}$ = 0.1/-0.7, beta $t_{max/min}$ = -0.3/-1.2, gamma $t_{max/min}$ = 0.0/-1.1).

strongest connections (10 percent edge density) and binarized. These graphs allow for summarizing local and global properties of complex networks with a few measures. We first examined the local properties of brain networks in chronic pain patients. A basic property of a node is the number of its connections to other nodes, which is termed the degree. Conceptually, the degree is closely related to the connectivity strength analyzed in the previous step, the essential difference being that the edges are thresholded, whereas the connectivity strength considers all connections. We computed the degree of every voxel and compared it between patients and controls. No difference in degree was found in any frequency band (Figure 17A and B). This applied similarly to phase-based and amplitude-based measures of connectivity (PLV: p_{min}(corrected/uncorrected) = 0.51/0.13, t_{max} = 4.2; AEC: p_{min}(corrected/uncorrected) = 1/0.56, t_{max} = 3.0). To further investigate this, we computed the weighted degree, i.e. a thresholded but not binarized connectivity matrix. The cluster-based permutation tests of the weighted degree in the theta and gamma bands showed no significant differences between patients and controls. This lack of a difference in degree indicates that the difference in connectivity strength is not confined to the strongest connections but instead applies to connections of all strengths. Another well-established measure that characterizes nodes is the clustering coefficient. This measure assesses the number of connections of neighboring nodes, i.e. it measures the local integration of a node served by short-range connectivity. Comparing the clustering coefficients of all nodes between patients and controls did not show any significant differences at any frequency band, neither for phase-based nor amplitude-based connectivity (Figure 17C and D; PLV: p_{min}(corrected/uncorrected) = 0.12/0.030, t_{max} = 3.3, AEC: p_{min}(corrected/uncorrected) = 1/0.28, t_{max} = 3.8).

Taken together, the analysis of local measures of functional connectivity showed

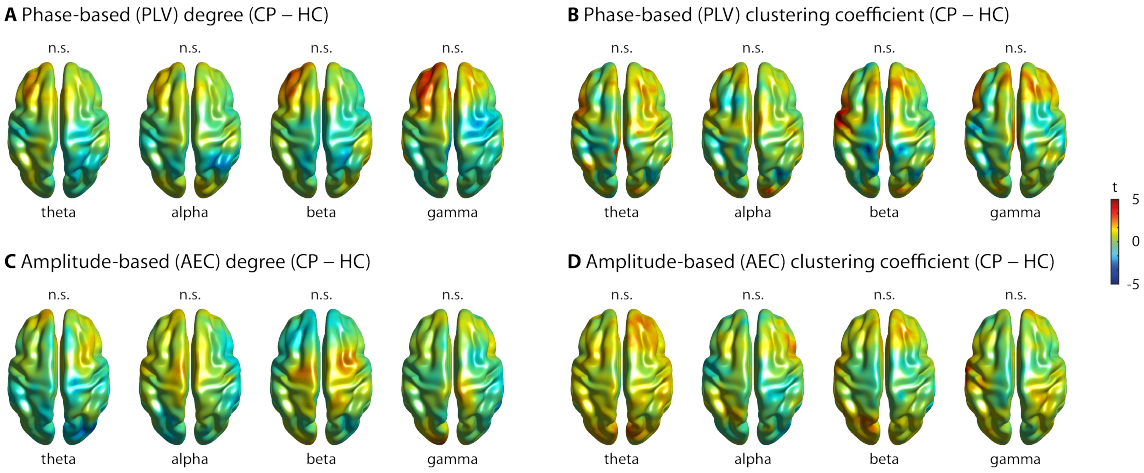

Figure 17: Local measures of functional connectivity - degree and local clustering coefficient.

Brain topographies of the comparison of degree and local clustering coefficient between chronic pain patients (CP) and healthy controls (HC) in the theta, alpha, beta and gamma band frequencies, averaged across frequencies in each band, are shown. The degree is the number of connections of a voxel, thresholded to the 10 percent highest connectivity values. The local clustering coefficient is a measure of how well a voxel's neighbors are connected. The colormaps show t-values. Cluster-based permutation tests were performed to test for significance. Significant results are masked, i.e. all voxels but the ones belonging to a significant cluster are greyed out. In the absence of significant clusters, colors were retained to show potential trends. Here, no significant effects were found and, thus, nothing is greyed out. (**A**) PLV-based degree. No significant difference between the degrees of chronic pain patients and healthy controls was observed in any frequency band (theta $t_{max/min}$ = 3.3/-3.8, alpha $t_{max/min}$ = 3.1/-3.4, beta $t_{max/min}$ = 3.7/-2.6, gamma $t_{max/min}$ = 4.2/-3.3). (**B**) PLV-based local clustering coefficient. No significant difference between the local clustering coefficients of chronic pain patients and healthy controls was observed in any frequency band (theta $t_{max/min}$ = 4.4/-2.9, alpha $t_{max/min}$ = 3.7/-3.3, beta $t_{max/min}$ = 4.5/-3.5, gamma $t_{max/min}$ = 3.6/-3.2). (**C**)AEC-based degree. No significant difference between the degrees of chronic pain patients and healthy controls was found in any frequency band (theta $t_{max/min}$ = 3.0/-3.2, alpha $t_{max/min}$ = 2.3/-2.6, beta $t_{max/min}$ = -2.6/-1.9, gamma $t_{max/min}$ = 3.2/-3.0). (**D**) AEC-based local clustering coefficient. No significant difference between the local clustering coefficients of chronic pain patients and healthy controls was observed in any frequency band (theta $t_{max/min}$ = 3.2/-1.5, alpha $t_{max/min}$ = 2.7/-2.7, beta $t_{max/min}$ = 3.5/-2.7, gamma $t_{max/min}$ = 3.8/-1.8).

increases of phase-based connectivity in frontal and prefrontal cortices at theta and gamma frequencies in chronic pain patients. The increase in the theta band was of small effect size (Cohen's d = 0.40), whereas the increase in the gamma band was of medium effect size (Cohen's d = 0.59).

3.4 Global Measures of Functional Connectivity

We next investigated whether chronic pain was associated with changes of global measures of functional connectivity and therefore computed graph measures which characterize different complementary global properties of brain networks. Figure 18 summarizes the results of the global graph measures. First, we calculated the global clustering coefficient, which is the average of the local clustering coefficient across the whole network. This is commonly interpreted as a measure of functional segregation in a network (Rubinov and Sporns, 2010; Fornito et al., 2016), i.e. how

specialized sub-regions of the brain are. We found no differences in global clustering coefficient between chronic pain patients and healthy controls (Table 4; p_{min} (corrected/uncorrected) = 0.088/0.022).

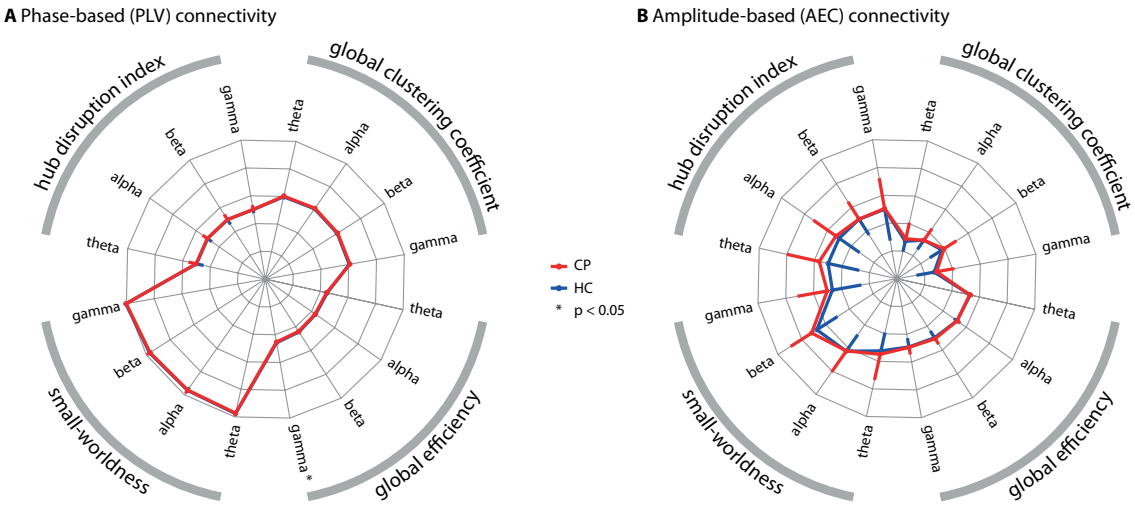

Figure 18: Global graph theoretical measures of functional connectivity.

The radar plots show four global graph measures in four frequency bands based on (A) PLV and (B) AEC-based connectivity measures. The clockwise arrangement follows the following pattern: theta, alpha, beta and gamma repeat within the arrangement of the four graph measures: global clustering coefficient, global efficiency, small-worldness and absolute values of the hub disruption index. The red lines show the chronic pain patients' (CP) values, while the blue lines represent the healthy controls' (HC). Error bars show the standard deviation. For visualization purposes, the symmetric error bars are only drawn in a single radial direction. Axes run from the center (= 0) to the outside (= 1). For visualization purposes, the small-worldness and hub disruption index were scaled with a factor of 0.2 and the absolute unsigned value is shown. (**A**) Phase-based connectivity (PLV). The global efficiency in the gamma band was significantly decreased in chronic pain patients (non-parametric permutation test, p(corrected/uncorrected) = 0.013/0.0032, Cohen's d = 0. 44). No other measure revealed a significant difference when compared between groups; see Table 4 for details. (**B**) Amplitude-based connectivity (AEC). No significant difference between groups was observed; see Table 4 for statistical details.

Second, we assessed the global efficiency, which is the mean of the inverse of the shortest path length between each pair of nodes. This measure provides an account of the ease of long-distance communication and is commonly interpreted as a measure of functional integration in a network (Rubinov and Sporns, 2010; Fornito et al., 2016). After accounting for multiple comparisons, we found evidence for a decrease of global efficiency in patients in the gamma frequency band when investigating phase-based connectivity (Table 4; p(corrected/uncorrected) = 0.013/0.0032). The effect size of this difference was small (Cohen's d = 0.44). Third, we computed the small-worldness, which combines the two aforementioned measures and compares it against a random network. This measure is associated with communication efficiency within a network (Rubinov and Sporns, 2010; Fornito et al., 2016). We detected no changes in small-worldness between the two groups (Table 2; p_{min}(corrected/uncorrected) = 0.26/0.064). Fourth, we analyzed the hub disruption index (Achard et al., 2012), which has been shown to differ between chronic

pain patients and controls in previous functional magnetic resonance imaging studies (Mano et al., 2018; Mansour et al., 2016). The hub disruption index compares the degree of all nodes to those of a control group. Positive values indicate that strongly connected nodes increase and weakly connected nodes decrease their number of connections ("the rich get richer and the poor get poorer"). Conversely, negative values indicate that strongly connected nodes decrease and weakly connected nodes increase their number of connections ("the rich get poorer and the poor get richer"), which means a shift of the network towards a random network with less internal structure. Our results did not show a difference of the hub disruption index in any frequency band when comparing chronic pain patients to healthy controls (Table 4; p_{min}(corrected/uncorrected) = 1/0.32).

In summary, global graph measures of phase-based functional connectivity showed a decrease of global efficiency at gamma frequencies in chronic pain patients. This decrease was of small effect size (Cohen's d = 0.44).

Table 4: Global graph measure statistics.

	PLV				AEC				dwPLI			
	θ	α	β	γ	θ	α	β	γ	θ	α	β	γ
gCC	0.084	0.040	0.092	0.022	0.22	0.92	0.29	0.38	0.088	0.45	0.017	0.47
gEff	0.052	0.13	0.084	0.0032	0.17	0.78	0.30	0.74	0.29	0.051	0.20	0.12
S	0.17	0.24	0.24	0.064	0.30	0.92	0.094	0.24	0.085	0.30	0.090	0.29
k_d	0.77	0.64	0.94	0.88	0.066	0.32	0.99	0.88	0.048	0.20	0.43	0.00

Uncorrected p-values of non-parametric permutation tests comparing global graph measures between groups. P-values were corrected for multiple comparisons using the Holm-Bonferroni method across the four frequency bands to take cross-spectral dependencies into account. After correction, the PLV-based global efficiency in the gamma band differed significantly between groups (p(corrected) = 0.013, Cohen's d = 0.44). The dwPLI-based hub disruption index (kd) in the gamma band was significantly lower in patients (p(corrected) = 0.00, Cohen's d = 0.63). Cell coloring indicates the direction of significant effects; blue indicates lower values in chronic pain patients. gCC, global clustering coefficient; gEff, global efficiency; S, small-worldness; k_d, hub disruption index.

3.5 Local and Global Measures of Functional Connectivity - dwPLI

We further tested whether changes of functional connectivity in chronic pain patients can be detected using another common phase-based connectivity measure, the dwPLI (30). The dwPLI differs from the PLV by capturing only non-zero phase lag connectivity. The dwPLI is therefore not susceptible to volume conduction which can yield artificial connectivity effects at the cost of reduced sensitivity because real synchrony at zero phase lag is also discarded. The results of the cluster-based permutation tests did not reveal any local difference in functional connectivity between patients and controls (Figure 19A – C, p_{min} (corrected/uncorrected) = 0.48/0.12, t_{min} = -3.0). This indicates that zero phase lag connectivity plays an important role in the increased frontal connectivity of patients. Concerning global graph measures (Figure 19 and Table 4), the hub disruption index was significantly lower in chronic

pain patients in the gamma band (p(corrected/uncorrected) = 0.00/0.00, Cohen's d = 0.63).

In summary, when the connectivity was calculated using the dwPLI, there was a decrease of the hub disruption index in chronic pain patients with a medium effect size (Cohen's d = 0.63), but no local connectivity differences could be found.

3.6 Control Analyses

As muscle artifacts may cause spurious synchrony, we computed a control analysis using the EMG electrodes on the right neck and masseter. We band-passed the signals from the neck and the masseter electrode in the theta and gamma frequency bands and then computed connectivity from each single EMG electrode to the peak voxel of the statistically significant clusters in the theta (MNI = [- 10 10 70]) and gamma (MNI = [- 40 40 30]) band, respectively. Afterwards, we tested the EMG connectivity of the chronic pain patients against the healthy controls' with a non-parametric permutation test. These tests revealed that no significant difference in EMG-to-peak voxel-connectivity could be detected.

We tested the robustness of the local and global graph measures against a change of the threshold responsible for creating the graphs, i.e. the edge density. We therefore repeated the analyses with edge densities of 5 and 20 percent (the initial edge density being 10 percent). As can be seen in Figure 20 and Figure 21, our negative findings were consistent across the different edge densities. At the same time, Table 5 and Table 6 show that the global graph measure effects in the gamma band were robust across edge densities as well.

In summary, the PLV global efficiency and the dwPLI hub disruption index in the gamma band were consistently changed in chronic pain patients. Both were decreased in chronic pain patients, with the PLV global efficiency showing a small effect size (average Cohen's d = 0.44) and the dwPLI hub disruption index showing a medium effect size (average Cohen's d = 0.61).

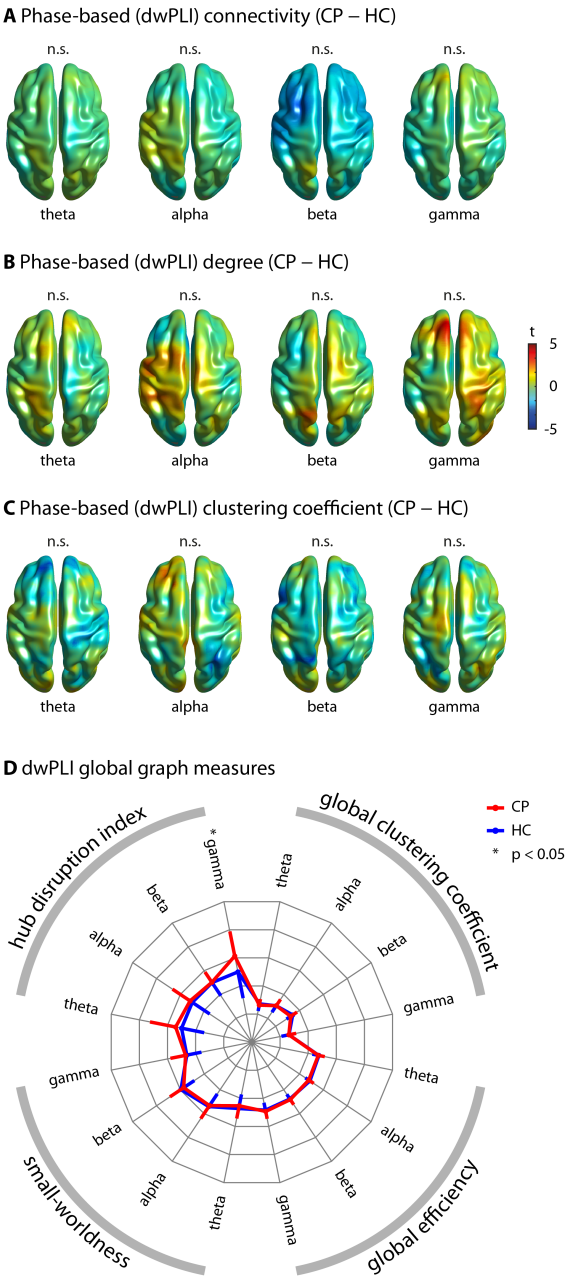

Figure 19: Local and global graph theoretical measures of functional connectivity - dwPLI.

All connectivity analyses based on the dwPLI, a more conservative phase-based connectivity measure. Brain topographies of the comparison of connectivity strength, degree and local clustering coefficient between chronic pain patients (CP) and healthy controls (HC) in the theta, alpha, beta and gamma band frequencies, averaged across frequencies in each band, are shown in (A) – (C). The colormaps show t-values. Cluster-based permutation tests were performed to test for significance. Significant results are masked, i.e. all voxels but the ones belonging to a significant cluster are greyed out. In the absence of significant clusters, colors were retained to show potential trends. No significant effects were found in the local connectivity analyses and, thus, nothing is greyed out. (**A**) dwPLI connectivity strength. No significant difference between the connectivity strength of chronic pain patients and healthy controls was observed in any frequency band (theta $t_{max/min}$ = 2.2/-2.3, alpha $t_{max/min}$ = 2.3/-3.0, beta $t_{max/min}$ = 1.2/-3.0, gamma $t_{max/min}$ = 1.6/-2.8). (**B**) dwPLI degree. No significant difference between the degrees of chronic pain patients and healthy controls was observed in any frequency band (theta $t_{max/min}$ = 2.9/-3.1, alpha $t_{max/min}$ = 4.2/-4.1, beta $t_{max/min}$ = 3.2/-2.5, gamma $t_{max/min}$ = 4.1/-3.4). (**C**) dwPLI clustering coefficient. No significant difference between the clustering coefficients of chronic pain patients and healthy controls was observed in any frequency band (theta $t_{max/min}$ = 2.8/-3.9, alpha $t_{max/min}$ = 3.1/-3.3, beta $t_{max/min}$ = 2.8/-4.0, gamma $t_{max/min}$ = 3.2/-3.2). (**D**) The radar plot is analogous to Figure 18. Here, global graph measures based on dwPLI connectivity are shown. Only the hub disruption index in the gamma band was significantly lower in chronic pain patients (p(corrected) = 0.00, Cohen's d = 0.63). No other global graph measure showed a significant difference, see Table 4 for statistical details.

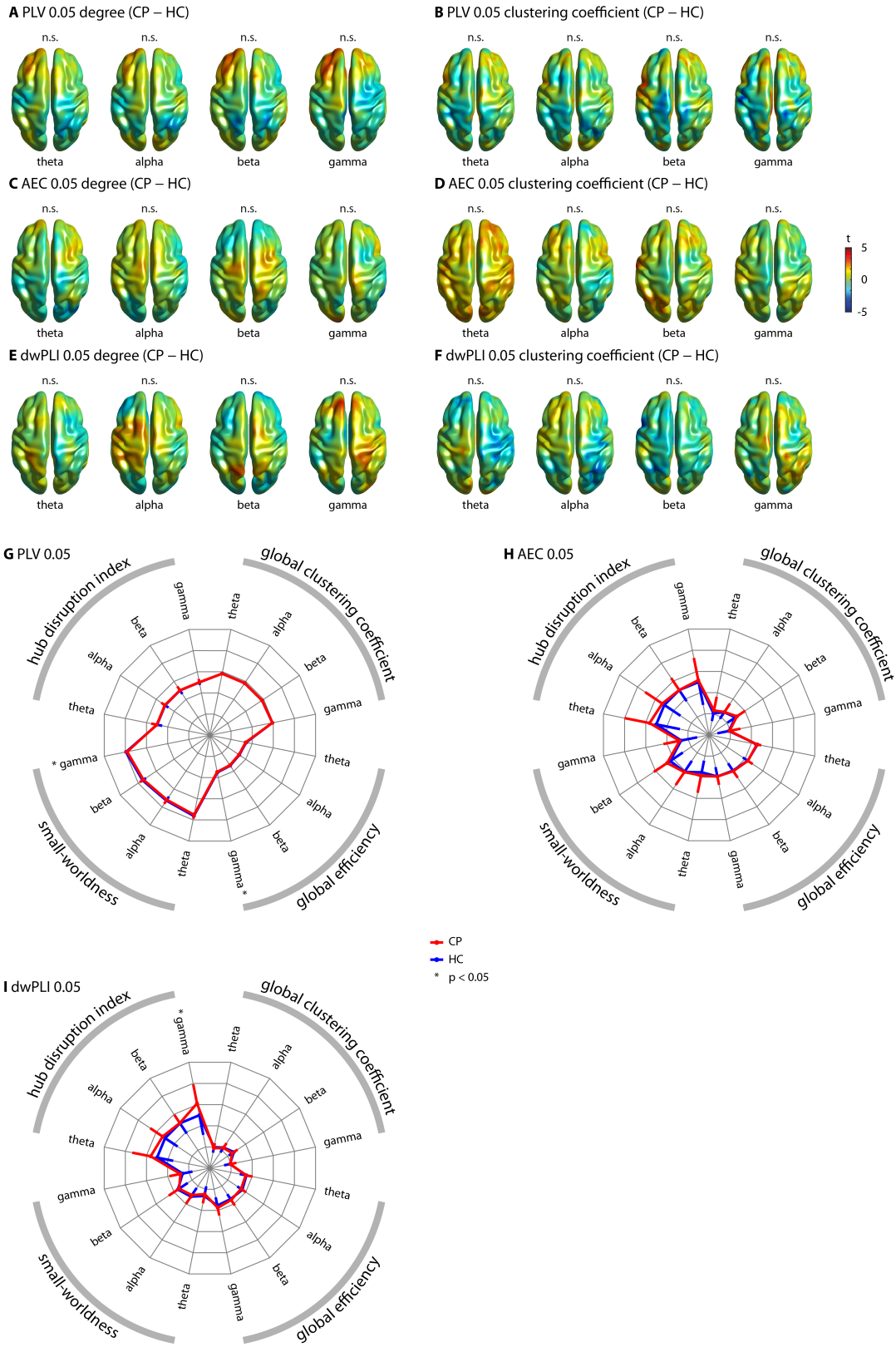

Figure 20: Local and global measures of functional connectivity – 5 percent edge density

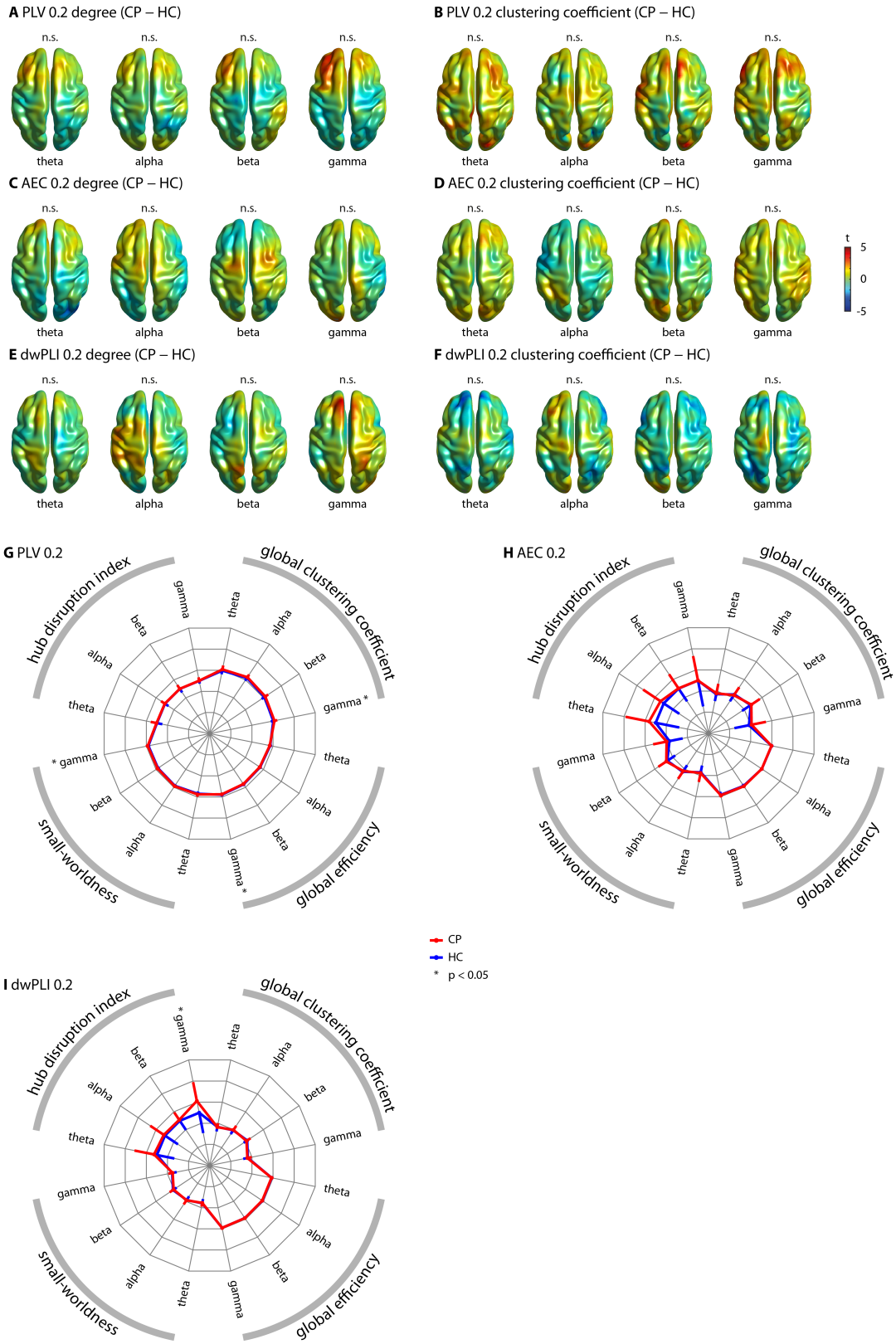

Figure 21: Local and global measures of functional connectivity – 20 percent edge density

In Figure 20 and Figure 21 graph analyses were repeated with an edge density of 5 percent instead of 10 percent, i.e. the threshold for edges within the graphs was set to the 5 percent highest connectivity values. (A) – (F) are analogous to Figure 17, showing the comparison of degree and clustering coefficient between chronic pain patients (CP) and healthy controls (HC).

Figure 20: (**A**) Degree based on PLV with 5 percent edge density. No significant difference between the degrees of chronic pain patients and healthy controls was observed in any frequency band (theta $t_{max/min}$ = 3.2/-3.5, alpha $t_{max/min}$ = 3.0/-3.2, beta $t_{max/min}$ = 3.7/-3.2, gamma $t_{max/min}$ = 3.8/-3.4). (**B**) PLV clustering coefficient with 5 percent edge density. No significant difference between the clustering coefficients of chronic pain patients and healthy controls was observed in any frequency band (theta $t_{max/min}$ = 4.0/-4.2, alpha $t_{max/min}$ = 3.3/-3.8, beta $t_{max/min}$ = 3.6/-3.9, gamma $t_{max/min}$ = 3.5/-4.2). (**C**) Degree based on AEC with 5 percent edge density. No significant difference between the degrees of chronic pain patients and healthy controls was observed in any frequency band (theta $t_{max/min}$ = 3.0/-2.7, alpha $t_{max/min}$ = 2.4/-2.9, beta $t_{max/min}$ = 2.5/-2.2, gamma $t_{max/min}$ = 3.0/-3.3). (**D**) AEC clustering coefficient with 5 percent edge density. No significant difference between the clustering coefficients of chronic pain patients and healthy controls was observed in any frequency band (theta $t_{max/min}$ = 3.5/-1.9, alpha $t_{max/min}$ = 2.5/-2.6, beta $t_{max/min}$ = 3.4/-2.7, gamma $t_{max/min}$ = 2.9/-2.4). (**E**) Degree based on dwPLI with 5 percent edge density. No significant difference between the degrees of chronic pain patients and healthy controls was observed in any frequency band (theta $t_{max/min}$ = 3.0/-3.3, alpha $t_{max/min}$ = 3.6/-4.2, beta $t_{max/min}$ = 3.6/-2.4, gamma $t_{max/min}$ = 3.4/-3.1). (**F**) dwPLI clustering coefficient with 5 percent edge density. No significant difference between the clustering coefficients of chronic pain patients and healthy controls was observed in any frequency band (theta $t_{max/min}$ = 2.8/-3.4, alpha $t_{max/min}$ = 3.0/-3.7, beta $t_{max/min}$ = 2.9/-4.3, gamma $t_{max/min}$ = 3.2/-2.6). (G) – (I) are radar plots analogous to Figure 18, for statistical details see Table 5. (**G**) PLV global graph measures based on 5 percent edge density. PLV-based global efficiency in the gamma band was significantly lower in patients (p(corrected) = 0.011, Cohen's d = 0.44). The PLV-based small-worldness in the gamma band was also significantly lower in patients (p(corrected) = 0.0040, Cohen's d = 0.45). (**H**) AEC global graph measures based on 5 percent edge density. No significant difference was found. (**I**) dwPLI global graph measures based on 5 percent edge density. dwPLI-based hub disruption index in the gamma band was significantly lower in patients (p(corrected) = 0.00, Cohen's d = 0.61).

Figure 21: (**A**) Degree based on PLV with 20 percent edge density. No significant difference between chronic pain patients' and healthy controls' degrees were observed in any frequency band (theta $t_{max/min}$ = 3.0/-3.6, alpha $t_{max/min}$ = 2.9/-3.0, beta $t_{max/min}$ = 3.7/-2.7, gamma $t_{max/min}$ = 3.9/-3.5). (**B**) PLV clustering coefficient with 20 percent edge density. No significant difference between chronic pain patients' and healthy controls' clustering coefficients were observed in any frequency band (theta $t_{max/min}$ = 4.1/-1.6, alpha $t_{max/min}$ = 3.2/-3.1, beta $t_{max/min}$ = 5.1/-2.4, gamma $t_{max/min}$ = 5.2/-1.9). (**C**) Degree based on AEC with 20 percent edge density. No significant difference between chronic pain patients' and healthy controls' degrees were observed in any frequency band (theta $t_{max/min}$ = 2.9/-3.4, alpha $t_{max/min}$ = 2.6/-2.7, beta $t_{max/min}$ = 2.6/-2.0, gamma $t_{max/min}$ = 3.3/-2.8). (**D**) AEC clustering coefficient with 20 percent edge density. No significant difference between chronic pain patients' and healthy controls' clustering coefficients were observed in any frequency band (theta $t_{max/min}$ = 2.9/-1.8, alpha $t_{max/min}$ = 2.1/-2.5, beta $t_{max/min}$ = 3.0/-2.0, gamma $t_{max/min}$ = 3.3/-1.1). (**E**) Degree based on dwPLI with 20 percent edge density. No significant difference between chronic pain patients' and healthy controls' degrees were observed in any frequency band (theta $t_{max/min}$ = 3.0/-2.8, alpha $t_{max/min}$ = 4.1/-3.8, beta $t_{max/min}$ = 3.2/-2.7, gamma $t_{max/min}$ = 4.1/-3.2). (**F**) dwPLI clustering coefficient with 20 percent edge density. No significant difference between chronic pain patients' and healthy controls' clustering coefficients were observed in any frequency band (theta $t_{max/min}$ = 2.7/-3.5, alpha $t_{max/min}$ = 2.9/-3.3, beta $t_{max/min}$ = 2.7/-3.4, gamma $t_{max/min}$ = 2.9/-3.6). (G) – (I) are radar plots analogous to Figure 18, for statistical details see Table 6. (**G**) PLV global graph measures based on 20 percent edge density. PLV-based global clustering coefficient in the gamma band was significantly higher in patients (p(corrected) = 0.014, Cohen's d = 0.0012). The PLV-based global efficiency in the gamma band was significantly lower in patients (p(corrected) = 0.0080, Cohen's d = 0.00040). The PLV-based small-worldness in the gamma band was significantly higher in patients (p(corrected) = 0.045, Cohen's d = 0.0036). (**H**) AEC global graph measures based on 20 percent edge density. No significant differences were found. (**I**) dwPLI global graph measures based on 20 percent edge density. dwPLI-based hub disruption index in the gamma band was significantly lower in patients (p(corrected) = 0.00, Cohen's d = 0.056).

Table 5: Global graph measure statistics – 5 percent edge density.

	PLV				AEC				dwPLI			
	θ	α	β	γ	θ	α	β	γ	θ	α	β	γ
gCC	0.31	0.44	0.46	0.27	0.049	0.42	0.10	0.35	0.097	0.33	0.017	0.38
gEff	0.026	0.082	0.038	0.0014	0.17	0.42	0.31	0.48	0.27	0.045	0.14	0.036
S	0.017	0.099	0.055	0.0005	0.081	0.46	0.058	0.27	0.10	0.13	0.22	0.089
k_d	0.38	0.31	0.46	0.38	0.032	0.19	0.50	0.30	0.0071	0.090	0.44	0.00

Uncorrected p-values of non-parametric permutation tests comparing global graph measures between chronic pain patients and healthy controls, based on voxels, but with 5 percent edge density, i.e. only the 5 percent highest connectivity values were included in the graph analyses. P-values were corrected for multiple comparisons using the Holm-Bonferroni method across the four frequency bands to take cross-spectral dependencies into account. After correction, the PLV-based global efficiency in the gamma band was significantly lower in patients (p(corrected) = 0.011, Cohen's d = 0.44). The PLV-based small-worldness in the gamma band was also significantly lower in patients (p(corrected) = 0.0040, Cohen's d = 0.45). Further, the dwPLI-based hub disruption index in the gamma band was also significantly lower in patients (p(corrected) = 0.00, Cohen's d = 0.61). Cell coloring indicates the direction of significant effects; blue indicates lower values in chronic pain patients. gCC, global clustering coefficient; gEff, global efficiency; S, small-worldness; kd, hub disruption index.

Table 6: Global graph measure statistics – 20 percent edge density.

	PLV				AEC				dwPLI			
	θ	α	β	γ	θ	α	β	γ	θ	α	β	γ
gCC	0.022	0.033	0.036	0.0018	0.25	0.25	0.30	0.12	0.34	0.27	0.12	0.24
gEff	0.024	0.090	0.050	0.0010	0.042	0.34	0.071	0.15	0.25	0.18	0.38	0.47
S	0.031	0.027	0.052	0.0056	0.27	0.25	0.21	0.073	0.27	0.35	0.14	0.25
k_d	0.32	0.39	0.45	0.36	0.029	0.093	0.45	0.50	0.15	0.29	0.24	0.00

Uncorrected p-values of non-parametric permutation tests comparing global graph measures between chronic pain patients and healthy controls, based on voxels, but with 20 percent edge density, i.e. only the 20 percent highest connectivity values were included in the graph analyses. P-values were corrected for multiple comparisons using the Holm-Bonferroni method across the four frequency bands to take cross-spectral dependencies into account. After correction, the PLV-based global clustering coefficient in the gamma band was significantly higher in patients (p(corrected) = 0.014, Cohen's d = 0.43). The PLV-based global efficiency in the gamma band was significantly lower in patients (p(corrected) = 0.0080, Cohen's d = 0.44). The PLV-based small-worldness in the gamma band was significantly higher in patients (p(corrected) = 0.045, Cohen's d = 0.38). Further, the dwPLI-based hub disruption index in the gamma band was also significantly lower in patients (p(corrected) = 0.00, Cohen's d = 0.61). Cell coloring indicates the direction of significant effects; blue and red indicate lower and higher values in chronic pain patients, respectively. gCC, global clustering coefficient; gEff, global efficiency; S, small-worldness; kd, hub disruption index.

3.7 Relationships Between Brain Activity and Clinical Parameters

We further investigated the relationships of brain-based activity and connectivity measures with clinical parameters. To reduce the number of statistical tests, we restricted our analyses to selected measures of brain activity and brain connectivity that were associated with clinical parameters of chronic pain patients in previous studies (Sarnthein et al., 2006; Stern et al., 2006; Schmidt et al., 2012; de Vries et al., 2013; Gonzalez-Roldan et al., 2016; Mansour et al., 2016; Kuo et al., 2017; Vanneste et al., 2017; Choe et al., 2018; Fallon et al., 2018). We thus computed correlations between the global peak frequency, mean global power in the four frequency bands,

the hub disruption index, and the following major clinical parameters: current pain intensity, average pain intensity in the last four weeks, pain duration, pain disability, mental and physical quality of life, depression, and medication as quantified by the medication quantification scale (Harden et al., 2005). Additionally, we correlated the significant clusters in the theta and gamma PLV connectivity, the PLV global efficiency in the gamma band, and the dwPLI hub disruption index with the same clinical parameters. The results showed no significant correlations (Figure 22). Thus, we did not observe any relationships between measures of brain activity and functional connectivity, and clinical parameters including medication. This suggests that frontal connectivity increases and global network changes in chronic pain patients do not scale with disease characteristics, but rather characterize the state of chronic pain per se.

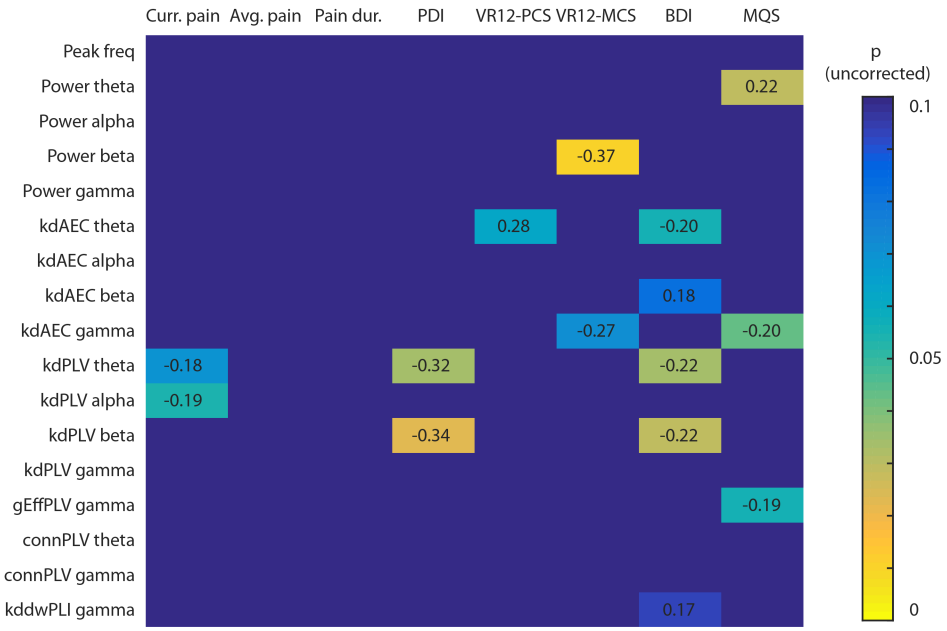

Figure 22: Correlations between clinical/behavioral parameters and brain activity/functional connectivity measures.

The cell values show the strength and direction of the correlations (Pearson's r) and the color depicts the uncorrected p values. Only correlations showing a trend ($p < 0.1$) are shown. No correlation was statistically significant after Holm-Bonferroni correction for multiple comparisons across the four frequency bands. Curr. pain, current pain intensity; Avg. pain, average pain intensity in the last 4 weeks; Pain dur., pain duration; PDI, pain disability index; VR12-PCS, Veterans's RAND physical component score; VR12-MCS, Veterans's RAND mental component score; BDI, Beck Depression Inventory II, MQS, medication quantification scale; peak freq, peak frequency; kd, hub disruption index; AEC, measure is based on the orthogonalized amplitude envelope correlation; PLV, measure is based on the phase locking value; dwPLI, measure is based on the debiased weighted phase lag index; gEff, global efficiency; conn, connectivity strength.

3.8 Machine Learning Approach

Finally, we performed a multivariate machine learning approach. This approach extends the previous univariate approaches by taking patterns of brain activity and connectivity into account rather than single pieces of information in isolation. Moreover, it complements the previous descriptive group analyses by adding a predictive, single-subject analysis. We used an SVM classifier to test whether patterns of brain activity and/or connectivity can distinguish between chronic pain patients and healthy controls. We trained a linear SVM on all aforementioned measures of brain activity and functional connectivity, using an automated sequential feature selection algorithm. The performance of the SVM was evaluated using a 10-fold cross-validation. The resulting mean accuracy was 57 ± 4 percent with a sensitivity of 60 ± 5 percent and a specificity of 57 ± 5 percent. To test whether this result exceeds chance level, we repeated the whole procedure with the same data but randomly shuffled labels of chronic pain patients and healthy controls. This resulted in a permutation distribution with 50 ± 5 percent accuracy. A non-parametric permutation test of the two accuracy distributions (Figure 23A) confirmed that the real model was significantly more accurate than random guessing ($p < 0.001$). Finally, we were interested to know which features of brain activity and/or connectivity were most relevant for the classification. The automatic feature selection picked on average 5.5 features for the SVMs. We therefore show the 5 most frequently picked features in Figure 23B. The most relevant features were phase-based connectivity measures in frontal brain areas at gamma (MNI: -40, 30, 40 and -30, 50, 10) and theta (MNI: -20, 50, 40) frequencies. These 3 features were chosen with a rate greater than 10 percent each, whereas all other features were picked with a rate of less than 10 percent.

Thus, a multivariate machine learning approach could statistically significantly distinguish between chronic pain patients and healthy controls based on EEG measures of brain activity and connectivity. In particular, frontal phase-based connectivity at theta and gamma frequencies provided important information for the classification.

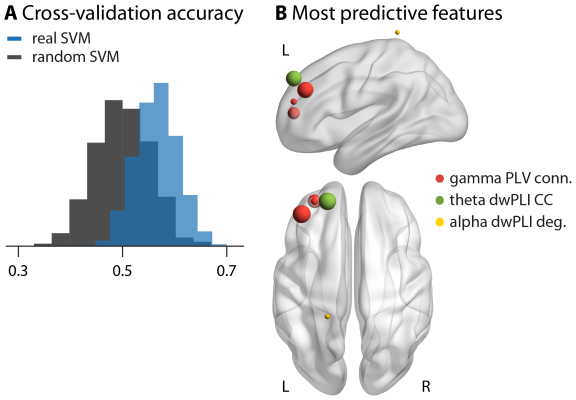

Figure 23: Multivariate machine learning approach to classify chronic pain patients and healthy controls.

(A) Distribution of mean accuracies resulting from a 10-fold cross-validation. The blue histogram shows the results trained on the actual data including all features of brain activity and connectivity. The gray histogram shows a SVM trained on data with randomly permuted labels. The SVM trained on the real data shows an accuracy of 57 $\pm$ 4 percent, significantly higher than the accuracy of the SVM trained on randomly permuted data, 50 $\pm$ 5 percent ($p < 0.001$). (B) The 5 most predictive features, i.e. those selected most consistently by the SVMs. Specific measures are color-coded; the size of the spheres represents how often a specific feature was selected. The most frequently selected features were PLV-based connectivity of the prefrontal cortex (MNI: -40, 30, 40 and -30, 50, 10) in the gamma band, which were selected in 15 percent and 12 percent of SVMs, respectively, and dwPLI-based connectivity of the prefrontal cortex (MNI: -20, 50, 40) in the theta band, which was selected in 15 percent of SVMs. All other features were selected with a frequency of less than 10 percent.

4 Discussion

In this study, we harnessed the potential of EEG to determine abnormalities of brain function in chronic pain. Defining such abnormalities promises to advance the understanding of the neural basis of chronic pain. Moreover, they might serve as a brain-based marker and novel treatment target of chronic pain. To this end, we recorded and compared resting-state EEG data of a large cohort of patients suffering from chronic pain with those of age and gender-matched healthy controls. The analyses ranged from well-established global measures of brain activity to sophisticated connectivity and network analyses in source space. All analyses were data-driven and rigorously corrected for multiple comparisons. To the best of our knowledge, this approach represents the most extensive analysis of EEG data from one of the largest cohorts of chronic pain patients so far. The results show that global measures of brain activity as measured by EEG did not differ between chronic pain patients and a matched healthy control group. However, our approach revealed a stronger phase-based connectivity at theta and gamma frequencies in the prefrontal cortex of chronic pain patients. Furthermore, we observed a global reorganization of brain networks at gamma frequencies. Based on patterns of brain activity and connectivity, a multivariate machine learning approach could classify chronic pain patients and healthy controls significantly above chance with an accuracy of 57 percent.

4.1 The TCD Model of Chronic Pain

Previous resting-state EEG studies investigating alterations in chronic pain patients mainly reported an increase in theta power together with a slowing of the global peak frequency compared to healthy controls (Sarnthein et al., 2006; Vanneste et al., 2018). These findings have been related to the Thalamocortical Dysrhythmia (TCD) model of chronic pain (Llinas et al., 2005). In this model, abnormal nociceptive input causes abnormal thalamic bursts at theta frequencies. These theta oscillations are transmitted to the cerebral cortex where they result in disinhibition of neighboring areas, which, in turn, results in abnormal oscillations at gamma frequencies and eventually in ongoing pain. This model is highly appealing, but evidence is still sparse (see 1.1.5 for an extensive review). The present completely data-driven approach in a large cohort of chronic pain patients neither shows increased theta power nor a shift of global peak frequency and therefore does not directly support the TCD model of chronic pain.

4.2 The Role of the Prefrontal Cortex in Chronic Pain

The univariate comparisons of brain activity/connectivity between groups and the multivariate machine learning approach congruently indicated increased functional connectivity of the prefrontal cortex in chronic pain patients. These findings are in accordance with fMRI studies (Baliki et al., 2012; Hashmi et al., 2013; Vachon-Presseau et al., 2016) as well as with recent reviews and theories (Seminowicz and Moayedi, 2017; Baliki and Apkarian, 2015; Rauschecker et al., 2015), which have shown that structural and functional alterations in the prefrontal cortex play an important role in chronic pain. Previous EEG studies have also pointed towards a close relationship between high-frequency oscillations in prefrontal areas and the perceived pain in chronic (May et al., 2018) and experimental longer-lasting pain (Nickel et al., 2017; Schulz et al., 2015), indicating a dissociation from the representation in sensorimotor areas that is generally observed in acute pain (Hu and Iannetti, 2019). A more precise localization of the connectivity increases in the prefrontal cortex is beyond the spatial resolution of EEG. Hence, it remains unclear how the present observations relate to the multitude of functions represented in the prefrontal cortex, which include motor, cognitive control, emotional, evaluative and modulatory functions (de la Vega et al., 2016; Kragel et al., 2018). However, a role of the prefrontal cortex in chronic pain points to an important function of emotional-evaluative, motivational and decision-making circuits rather than sensory circuits in chronic pain (Baliki and Apkarian, 2015; Rauschecker et al., 2015).

4.3 Brain Oscillations at Gamma Frequencies in Chronic Pain

Our findings revealed that chronic pain is associated with local increases of connectivity at gamma frequencies in the frontal cortex. These local increases were associated with a global disturbance of brain network organization in the gamma frequency band. The machine learning approach specifies that the frontal increase in connectivity of gamma oscillations has the highest predictive value for distinguishing chronic pain patients from healthy controls. Mechanistically, gamma oscillations have been related to the activity of inhibitory parvalbumin-positive GABAergic interneurons (Buzsaki and Wang, 2012). In an animal model of chronic pain, these interneurons have been implicated in the modulation of pyramidal cell firing in the prefrontal cortex and pain behavior (Zhang et al., 2015). This link between GABAergic inhibition, gamma oscillations, prefrontal cortex activity and pain behavior is in accordance with the present observations. Functionally, gamma oscillations have been associated with a broad range of cognitive and behavioral functions including object representation, memory and attention (Wang, 2010; Donner and Siegel, 2011; Fries, 2015). Thus, they likely represent a basic feature of neuronal signaling and

communication (Wang, 2010; Donner and Siegel, 2011; Fries, 2015), which appears to be particularly related to the local processing and feedforward communication of currently important stimuli (Ploner et al., 2017; Donner and Siegel, 2011; Fries, 2015). These concepts would be in line with an association of chronic pain with prefrontal gamma oscillations possibly signaling the emotional, motivational and evaluative aspects of pain.

4.4 Automated Classification of Chronic Pain

The multivariate machine learning approach showed that applying an SVM classifier to resting-state EEG data makes it possible to distinguish between chronic pain patients and healthy controls with a 57 percent accuracy. Interestingly, a recent study which pursued a closely related EEG approach showed accuracies of greater than 90 percent for the classification of chronic pain patients vs. healthy controls (Vanneste et al., 2018), which were not achieved in the present study. The reasons for this disparity remain unclear as the available information on the previous approach does not allow for precise replication. An attempted replication of the study's methods on our data with reasonable parameters did not yield a classification accuracy significantly above chance level.

Our machine learning approach identified features of brain activity which were particularly relevant for the distinction between chronic pain patients and healthy controls. In this study, we found that prefrontal connectivity at gamma frequencies (> 60 Hz) was particularly useful for the distinction between chronic pain patients and healthy controls. Interestingly, the automated feature selection chose on average only five to six features for the classification, indicating that additional features did not improve performance. This implies that many of the features contained redundant information, which may be a result of the spatial resolution of the source reconstructed EEG data being coarser than the chosen grid of 1 x 1 x 1 cm^3 voxels. Further, though we found no significant effects for the local connectivity using the dwPLI, two of the five most predictive features were dwPLI-based features. This indicates that the dwPLI connectivity measures also contained predictive information for the classification of chronic pain patients, albeit less than the PLV connectivity measures.

4.5 Altered Phase-based Connectivity in Chronic Pain

Thus, both phase-based connectivity measures, the dwPLI and PLV, showed predictive value in the multivariate approach and also revealed group-level differences in the univariate approach. We investigated both phase- and amplitude-based functional connectivity measures, and found no evidence for any alterations using the amplitude-based AEC measure. Intrinsic phase-based coupling has been shown to

be closely related to plasticity (Engel et al., 2013), being involved in shaping the cortical network during development (Uhlhaas et al., 2010) and memory processing in the adult brain (Fell and Axmacher, 2011). Thus, our results are consistent with models of chronic pain which are based on aberrant learning processes (Baliki and Apkarian, 2015; Seymour, 2019).

4.6 Limitations

Several limitations of the present study need to be pointed out. First, abnormal oscillations and synchrony are observed in many neurological diseases (Uhlhaas and Singer, 2006) and the specificity of the present results for chronic pain remains unclear. However, a potential lack of specificity does not necessarily limit the clinical usefulness and validity of a brain-based marker of chronic pain. In fact, many well-established laboratory, electrophysiological and imaging tests yield results which are neither disease-specific nor symptom-specific, but are clinically highly useful. A prominent example is C-reactive protein (CRP), an unspecific inflammatory marker ubiquitously used in various medical disciplines such as pulmonology (Butler et al., 2019) and cardiology (Danesh et al., 2004). Second, the temporal resolution of EEG is excellent, but its spatial resolution is low. The integration of the spatially highly resolved information from fMRI with the temporal information provided by EEG might therefore be a promising way to increase the accuracy of the present approach. Third, drug effects cannot be ultimately ruled out. We excluded patients taking benzodiazepines, which have known effects on EEG signals (Bauer and Bauer, 2011). However, in our representative cohort of chronic pain patients, most patients took non-opioid analgesics, opioids and/or antidepressants. To control for drug effects, we quantified medication using the medication quantification scale and found no significant correlations between medication and the observed EEG effects. Therefore, it is unlikely that our effects are solely driven by drug regimen. Fourth, field spread and/or muscle artifacts can cause spurious synchrony of EEG signals. A rigorous artifact correction procedure and analysis in source space are best practice to reduce these effects. Additionally, we have computed a control analysis with the connectivity between the peak voxels of our significant clusters and the EMG electrodes in the right neck and masseter to check whether our effects were driven solely by muscle artifacts and found no significant effect for the EMG signals. However, muscle artifacts remain an inherent and delicate confound of EEG signals.

4.7 Towards a Brain-based Marker of Chronic Pain

In conclusion, our extensive, data-driven, and systematic analysis of EEG data from a large cohort of chronic pain patients shows that global measures of brain activity did not differ between chronic pain patients and a healthy control group. These

negative findings might help to clarify inconsistencies in previous studies and guide future research. Our study reveals increased prefrontal synchrony together with global network reorganization at gamma frequencies in chronic pain, which enables differentiation between chronic pain patients and healthy controls. This finding advances the understanding of the brain mechanisms of chronic pain and might represent a step closer towards a safe, low-cost, widely available and potentially mobile brain-based marker of pain.

However, it is important to note that not all 7 criteria as established by the consensus paper (see 1.3) are met, and we can therefore not claim to have found a neuromarker of chronic pain.

1. Precise definition of a pain neuromarker. Using the SVM weights allows for a precise definition of a neuromarker and the SVM model also defines a precise threshold for classification. This criterion is therefore fulfilled.

2. Applicability of the pain neuromarker to individuals. As the SVM model is easily used to classify new datasets, this criterion is also fulfilled, albeit the accuracy is not sufficient for clinical use.

3. Methodological procedures used during testing must be validated. Recording resting-state EEG data is a well-established procedure, but preprocessing of EEG data depends largely on visual inspection. This makes standardization across different labs or hospitals challenging, making this criterion an issue of general importance for any EEG neuromarker.

4. Measures must be internally consistent and image data quality validated for the individual tested using positive and negative controls. In EEG data acquisition, many artifacts such as eye blinks and muscle activity are easily observed in the raw data, and can be controlled for during the recording or afterwards during preprocessing, but no established measure for data quality exists. It is therefore challenging to fulfill this criterion at the current state of EEG research.

5. The neuromarker must be diagnostic for pain. The largest caveat of our current putative neuromarker for chronic pain is its low accuracy, rendering it infeasible for clinical purposes. This criterion is therefore clearly not met.

6. The neuromarker must be validated with converging methods. Prefrontal regions have been implicated in fMRI studies of chronic pain patients (Kuner and Flor, 2017), and brain oscillations at gamma frequencies have also been associated with chronic pain in mouse models (Tan et al., 2019). Our results are therefore consistent across other neuroimaging methods and species.

7. The neuromarker must be generalizable to the patient group tested and to the test conditions. One of our goals was to find an overarching pattern across various types of chronic pain instead of one specific condition such as chronic back pain. We therefore investigated a large cohort suffering from diverse types of chronic pain. An important test of generalizability would be to apply our machine learning

model on an independent population of chronic pain patients and healthy controls to conclusively fulfill this criterion.

Thus, substantial challenges concerning the accuracy, specificity and generalizability of the findings remain to be overcome. Even though the accuracy of the present study is far from being sufficient for clinical purposes, this result has important implications. First, the present approach constitutes a proof-of-principle, showing that patterns of brain activity as measured by EEG can help distinguish chronic pain patients from healthy controls using a simple linear SVM. This represents a further step towards a much sought-after brain-based marker of pain (Davis et al., 2017; Upadhyay et al., 2018). FMRI recordings have already shown that, in principle, it is possible to establish such a marker (Wager et al., 2013; Mano et al., 2018). The present approach complements these fMRI approaches by using EEG recordings. Second, abnormal patterns of EEG activity in chronic pain might represent potential targets for novel therapeutic strategies such as non-invasive brain stimulation techniques (Polania et al., 2018) and/or neurofeedback approaches (Sitaram et al., 2017). In particular, the emerging transcranial alternating current stimulation (tACS) technique (Polania et al., 2018) allows for the frequency-specific modulation of neuronal oscillations and synchrony and might thus represent a promising approach to modulating pain. These results can therefore be seen as a localizer for future studies seeking to manipulate chronic pain via non-invasive brain stimulation.

Future projects which investigate the temporal variability of the EEG signals (Garrett et al., 2013) or implement deep learning (LeCun et al., 2015) might increase accuracy and specificity, and have already been started by our working group. Further, experiments in which prefrontal oscillations at gamma frequencies are modulated externally via tACS to modulate pain perception are also being conducted. These experiments could corroborate the current findings, advance our knowledge towards a brain-based marker of chronic pain, and provide causal evidence for the role of brain oscillations in pain perception. Importantly, any negative findings from these experiments, which are notoriously under-reported in general, would still contribute to our mechanistic understanding of pain and its processing in the brain. Other important next steps towards a brain-based marker of chronic pain are recordings from larger cohorts of patients with different types of chronic pain, comparisons with patients suffering from other neuropsychiatric diseases, the standardization of recording and analysis methods, and data-sharing approaches. These steps hold great promise but require huge concerted efforts. However, the enormous relevance of the clinical problem and the failure of many previous diagnostic and therapeutic strategies justify these efforts.

Acknowledgements

My most profound thanks go to the members of the Painlab Munich. First and foremost, thanks to my PhD supervisor Markus Ploner, who enabled my work to begin with and who was always supportive and helpful in both my actual work and any personal development such as conferences and workshops. All the other group members, Laura Bok, Elisabeth May, Moritz Nickel, Henrik Heitmann, Vanessa Hohn and Martina Postorino also deserve a special mention. Thanks go to Laura for her untiring ability to resolve all bureaucratic problems within minutes and her eye for the big picture, as well as for perpetually spreading her good mood. Thanks go to Elisabeth for her meticulous care of the office plants and her incredible precision and rigor when correcting manuscripts, as well as her caring empathy under any circumstances. Thanks go to Moritz for his great feedback and eye for details when dealing with new methodology, as well as the countless interesting discussions about various topics. Thanks go to Henrik for his vast medical and pharmaceutical knowledge and his unending efforts, as well as his amazingly entertaining stories and impressions. Thanks go to Vanessa for her great writing and online shopping skills, as well as the countless funny and entertaining stories. Thanks also go to Martina for establishing my first contact with the Painlab and her eternal friendliness, as well as her delicious desserts.

I kindly thank all patients and healthy participants for their participation in the study. Special thanks to Christine Berger and Vesna Dolanjski for support with patients and Marlene Försterling for help with the data acquisition. I also thank Paul Sauseng and Valentin Riedl, members of my thesis advisory committee for their helpful comments and the friendly meetings, as well as Joachim Gross for his competent and timely advice. Thanks to my various proofreaders, Laura, Moritz, Vanessa, Beth, and Sophia, as well.

Additionally, I would like to thank all past and current members of the TUM-NIC, in particular the many friends I have made through this collobarative institution. The kitchen was always a refuge from cerebral overheating and at the same a creative hotspot for all kinds of funny, interesting, or sometimes just silly ideas. Special mention goes to the AG Mühlau for the close partnership, especially during lunch. I have learned many things and enjoyed my time very much, thank you everybody!

References

Achard, S. and Bullmore, E. (2007). Efficiency and cost of economical brain functional networks. *PLoS Comput Biol*, 3(2):e17.

Achard, S., Delon-Martin, C., Vertes, P. E., Renard, F., Schenck, M., Schneider, F., Heinrich, C., Kremer, S., and Bullmore, E. T. (2012). Hubs of brain functional networks are radically reorganized in comatose patients. *Proc Natl Acad Sci U S A*, 109(50):20608–13.

Alpaydin, E. (2014). *Introduction to machine learning*. MIT press.

Apkarian, A. V., Bushnell, M. C., Treede, R. D., and Zubieta, J. K. (2005). Human brain mechanisms of pain perception and regulation in health and disease. *Eur J Pain*, 9(4):463–84.

Apkarian, A. V., Sosa, Y., Sonty, S., Levy, R. M., Harden, R. N., Parrish, T. B., and Gitelman, D. R. (2004). Chronic back pain is associated with decreased prefrontal and thalamic gray matter density. *J Neurosci*, 24(46):10410–5.

Azevedo, F. A., Carvalho, L. R., Grinberg, L. T., Farfel, J. M., Ferretti, R. E., Leite, R. E., Jacob Filho, W., Lent, R., and Herculano-Houzel, S. (2009). Equal numbers of neuronal and nonneuronal cells make the human brain an isometrically scaled-up primate brain. *J Comp Neurol*, 513(5):532–41.

Badhwar, A., Tam, A., Dansereau, C., Orban, P., Hoffstaedter, F., and Bellec, P. (2017). Resting-state network dysfunction in alzheimer's disease: A systematic review and meta-analysis. *Alzheimers Dement (Amst)*, 8:73–85.

Baker, J. T., Dillon, D. G., Patrick, L. M., Roffman, J. L., Brady, R. O., J., Pizzagalli, D. A., Ongur, D., and Holmes, A. J. (2019). Functional connectomics of affective and psychotic pathology. *Proc Natl Acad Sci U S A*, 116(18):9050–9059.

Baker, M. (2016). 1,500 scientists lift the lid on reproducibility. *Nature*, 533(7604):452–4.

Baliki, M. N. and Apkarian, A. V. (2015). Nociception, pain, negative moods, and behavior selection. *Neuron*, 87(3):474–91.

Baliki, M. N., Geha, P. Y., Apkarian, A. V., and Chialvo, D. R. (2008). Beyond feeling: chronic pain hurts the brain, disrupting the default-mode network dynamics. *J Neurosci*, 28(6):1398–403.

Baliki, M. N., Petre, B., Torbey, S., Herrmann, K. M., Huang, L., Schnitzer, T. J., Fields, H. L., and Apkarian, A. V. (2012). Corticostriatal functional connectivity predicts transition to chronic back pain. *Nat Neurosci*, 15(8):1117–9.

Basbaum, A. I., Bautista, D. M., Scherrer, G., and Julius, D. (2009). Cellular and molecular mechanisms of pain. *Cell*, 139(2):267–84.

Bassett, D. S. and Bullmore, E. (2006). Small-world brain networks. *Neuroscientist*, 12(6):512–23.

Bauer, G. and Bauer, R. (2011). *EEG, drug effects, and central nervous system poisoning*, pages 901–922. Oxford University Press, Philadelphia.

Bazanova, O. M. and Vernon, D. (2014). Interpreting eeg alpha activity. *Neurosci Biobehav Rev*, 44:94–110.

Bear, M. F., Connors, B. W., and Paradiso, M. A. (2016). *Neuroscience : exploring the brain*. Wolters Kluwer, Philadelphia, fourth edition. edition.

Beck, A. T., Steer, R. A., and Brown, G. (1996). *Manual for the Beck Depression Inventory-II*. TX: Psychological Corporation, San Antonio.

Bennett, D. L. and Woods, C. G. (2014). Painful and painless channelopathies. *Lancet Neurol*, 13(6):587–99.

Bishop, C. M. (2006). *Pattern recognition and machine learning*. springer.

Boord, P., Siddall, P. J., Tran, Y., Herbert, D., Middleton, J., and Craig, A. (2008). Electroencephalographic slowing and reduced reactivity in neuropathic pain following spinal cord injury. *Spinal Cord*, 46(2):118–23.

Breivik, H., Collett, B., Ventafridda, V., Cohen, R., and Gallacher, D. (2006). Survey of chronic pain in europe: prevalence, impact on daily life, and treatment. *Eur J Pain*, 10(4):287–333.

Buckner, R. L., Andrews-Hanna, J. R., and Schacter, D. L. (2008). The brain's default network: anatomy, function, and relevance to disease. *Ann N Y Acad Sci*, 1124:1–38.

Bullmore, E. and Sporns, O. (2009). Complex brain networks: graph theoretical analysis of structural and functional systems. *Nat Rev Neurosci*, 10(3):186–98.

Bushnell, M. C., Ceko, M., and Low, L. A. (2013). Cognitive and emotional control of pain and its disruption in chronic pain. *Nat Rev Neurosci*, 14(7):502–11.

Butler, C. C., Gillespie, D., White, P., Bates, J., Lowe, R., Thomas-Jones, E., Wootton, M., Hood, K., Phillips, R., Melbye, H., Llor, C., Cals, J. W., Naik, G., Kirby, N., Gal, M., Riga, E., and Francis, N. A. (2019). C-reactive protein testing to guide antibiotic prescribing for copd exacerbations. *New England Journal of Medicine*, 381(2):111–120.

Buzsaki, G. (2006). *Rhythms of the brain*. Oxford University Press, Oxford ; New York.

Buzsaki, G. and Wang, X. J. (2012). Mechanisms of gamma oscillations. *Annu Rev Neurosci*, 35:203–25.

Cardin, J. A., Carlen, M., Meletis, K., Knoblich, U., Zhang, F., Deisseroth, K., Tsai, L. H., and Moore, C. I. (2009). Driving fast-spiking cells induces gamma rhythm and controls sensory responses. *Nature*, 459(7247):663–7.

Cervero, F. and Laird, J. (1991). One pain or many pains? *News in Physiological Sciences*.

Choe, M. K., Lim, M., Kim, J. S., Lee, D. S., and Chung, C. K. (2018). Disrupted resting state network of fibromyalgia in theta frequency. *Sci Rep*, 8(1):2064.

Chu, C. J., Kramer, M. A., Pathmanathan, J., Bianchi, M. T., Westover, M. B., Wizon, L., and Cash, S. S. (2012). Emergence of stable functional networks in long-term human electroencephalography. *J Neurosci*, 32(8):2703–13.

Clauw, D. J. (2014). Fibromyalgia: a clinical review. *JAMA*, 311(15):1547–55.

Corder, G., Ahanonu, B., Grewe, B. F., Wang, D., Schnitzer, M. J., and Scherrer, G. (2019). An amygdalar neural ensemble that encodes the unpleasantness of pain. *Science*.

Cortes, C. and Vapnik, V. (1995). Support-vector networks. *Machine Learning*.

Costa Lda, C., Maher, C. G., McAuley, J. H., Hancock, M. J., Herbert, R. D., Refshauge, K. M., and Henschke, N. (2009). Prognosis for patients with chronic low back pain: inception cohort study. *BMJ*, 339:b3829.

da Silva, F. L. (2009). Eeg: Origin and measurement. pages 19–38.

Damoiseaux, J. S., Rombouts, S. A., Barkhof, F., Scheltens, P., Stam, C. J., Smith, S. M., and Beckmann, C. F. (2006). Consistent resting-state networks across healthy subjects. *Proc Natl Acad Sci U S A*, 103(37):13848–53.

Danesh, J., Wheeler, J. G., Hirschfield, G. M., Eda, S., Eiriksdottir, G., Rumley, A., Lowe, G. D., Pepys, M. B., and Gudnason, V. (2004). C-reactive protein and other circulating markers of inflammation in the prediction of coronary heart disease. *New England Journal of Medicine*, 350(14):1387–1397. PMID: 15070788.

Davis, K. D., Flor, H., Greely, H. T., Iannetti, G. D., Mackey, S., Ploner, M., Pustilnik, A., Tracey, I., Treede, R. D., and Wager, T. D. (2017). Brain imaging tests for chronic pain: medical, legal and ethical issues and recommendations. *Nat Rev Neurol*, 13:624–638.

de la Vega, A., Chang, L. J., Banich, M. T., Wager, T. D., and Yarkoni, T. (2016). Large-scale meta-analysis of human medial frontal cortex reveals tripartite functional organization. *J Neurosci*, 36(24):6553–62.

de Vries, M., Wilder-Smith, O. H., Jongsma, M. L., van den Broeke, E. N., Arns, M., van Goor, H., and van Rijn, C. M. (2013). Altered resting state eeg in chronic pancreatitis patients: toward a marker for chronic pain. *J Pain Res*, 6:815–24.

Denk, F., Bennett, D. L., and McMahon, S. B. (2017). Nerve growth factor and pain mechanisms. *Annu Rev Neurosci*, 40:307–325.

Di Pietro, F., Macey, P. M., Rae, C. D., Alshelh, Z., Macefield, V. G., Vickers, E. R., and Henderson, L. A. (2018). The relationship between thalamic gaba content and resting cortical rhythm in neuropathic pain. *Hum Brain Mapp*, page doi: 10.1007/hbm.23973.

Dillmann, U., Nilges, P., Saile, H., and Gerbershagen, H. U. (1994). [assessing disability in chronic pain patients.]. *Schmerz*, 8(2):100–10.

Donner, T. H. and Siegel, M. (2011). A framework for local cortical oscillation patterns. *Trends Cogn Sci*, 15(5):191–9.

Engel, A. K., Gerloff, C., Hilgetag, C. C., and Nolte, G. (2013). Intrinsic coupling modes: multiscale interactions in ongoing brain activity. *Neuron*, 80(4):867–86.

Fallon, N., Chiu, Y., Nurmikko, T., and Stancak, A. (2018). Altered theta oscillations in resting eeg of fibromyalgia syndrome patients. *Eur J Pain*, 22(1):49–57.

FDA-NIH Biomarker Working Group (2016). Best (biomarkers, endpoints, and other tools).

Fell, J. and Axmacher, N. (2011). The role of phase synchronization in memory processes. *Nat Rev Neurosci*, 12(2):105–18.

Fornito, A., Zalesky, A., and Bullmore, E. T. (2016). *Chapter 8 - Motifs, Small Worlds, and Network Economy*, pages 257–301. Academic Press, San Diego.

Fox, M. D. and Raichle, M. E. (2007). Spontaneous fluctuations in brain activity observed with functional magnetic resonance imaging. *Nat Rev Neurosci*, 8(9):700–11.

Freynhagen, R., Baron, R., Gockel, U., and Tolle, T. R. (2006). paindetect: a new screening questionnaire to identify neuropathic components in patients with back pain. *Curr Med Res Opin*, 22(10):1911–20.

Fries, P. (2015). Rhythms for cognition: Communication through coherence. *Neuron*, 88(1):220–35.

Furman, A. J., Meeker, T. J., Rietschel, J. C., Yoo, S., Muthulingam, J., Prokhorenko, M., Keaser, M. L., Goodman, R. N., Mazaheri, A., and Seminowicz, D. A. (2017). Cerebral peak alpha frequency predicts individual differences in pain sensitivity. *Neuroimage*, 167:203–210.

Garcia-Larrea, L., Frot, M., and Valeriani, M. (2003). Brain generators of laser-evoked potentials: from dipoles to functional significance. *Neurophysiol Clin*, 33(6):279–92.

Garrett, D. D., Samanez-Larkin, G. R., MacDonald, S. W., Lindenberger, U., McIntosh, A. R., and Grady, C. L. (2013). Moment-to-moment brain signal variability: a next frontier in human brain mapping? *Neurosci Biobehav Rev*, 37(4):610–24.

Geha, P. Y., Baliki, M. N., Harden, R. N., Bauer, W. R., Parrish, T. B., and Apkarian, A. V. (2008). The brain in chronic crps pain: abnormal gray-white matter interactions in emotional and autonomic regions. *Neuron*, 60(4):570–81.

Global Burden of Disease Study, C. (2017). Global, regional, and national incidence, prevalence, and years lived with disability for 328 diseases and injuries for 195 countries, 1990-2016: a systematic analysis for the global burden of disease study 2016. *Lancet*, 390(10100):1211–1259.

Gonzalez-Roldan, A. M., Cifre, I., Sitges, C., and Montoya, P. (2016). Altered dynamic of eeg oscillations in fibromyalgia patients at rest. *Pain Med*.

Gonzalez-Villar, A. J., Samartin-Veiga, N., Arias, M., and Carrillo-de-la Pena, M. T. (2017). Increased neural noise and impaired brain synchronization in fibromyalgia patients during cognitive interference. *Sci Rep*, 7(1):5841.

Gross, J., Schnitzler, A., Timmermann, L., and Ploner, M. (2007). Gamma oscillations in human primary somatosensory cortex reflect pain perception. *PLoS Biol*, 5(5):e133.

Harden, R. N., Weinland, S. R., Remble, T. A., Houle, T. T., Colio, S., Steedman, S., and Kee, W. G. (2005). Medication quantification scale version iii: update in medication classes and revised detriment weights by survey of american pain society physicians. *J Pain*, 6(6):364–71.

Hashmi, J. A., Baliki, M. N., Huang, L., Baria, A. T., Torbey, S., Hermann, K. M., Schnitzer, T. J., and Apkarian, A. V. (2013). Shape shifting pain: chronification of back pain shifts brain representation from nociceptive to emotional circuits. *Brain*, 136(Pt 9):2751–68.

Hauck, M., Lorenz, J., and Engel, A. K. (2007). Attention to painful stimulation enhances gamma-band activity and synchronization in human sensorimotor cortex. *J Neurosci*, 27(35):9270–7.

Henschke, N., Maher, C. G., Refshauge, K. M., Herbert, R. D., Cumming, R. G., Bleasel, J., York, J., Das, A., and McAuley, J. H. (2008). Prognosis in patients with recent onset low back pain in australian primary care: inception cohort study. *BMJ*, 337:a171.

Hipp, J. F., Hawellek, D. J., Corbetta, M., Siegel, M., and Engel, A. K. (2012). Large-scale cortical correlation structure of spontaneous oscillatory activity. *Nat Neurosci*, 15(6):884–90.

Hodgkin, A. L. and Huxley, A. F. (1952). A quantitative description of membrane current and its application to conduction and excitation in nerve. *J Physiol*, 117(4):500–44.

Holm, S. (1979). A simple sequentially rejective multiple test procedure. *Scand J Statist*, 6:65–70.

Hu, L. and Iannetti, G. D. (2016). Painful issues in pain prediction. *Trends Neurosci*.

Hu, L. and Iannetti, G. D. (2019). Neural indicators of perceptual variability of pain across species. *Proc Natl Acad Sci U S A*.

Hucho, T. and Levine, J. D. (2007). Signaling pathways in sensitization: toward a nociceptor cell biology. *Neuron*, 55(3):365–76.

Humphries, M. D. and Gurney, K. (2008). Network 'small-world-ness': a quantitative method for determining canonical network equivalence. *PLoS One*, 3(4):e0002051.

Institute of Medicine of the National Academies (2011). Relieving pain in america: A blueprint for transforming prevention, care, education, and research [report brief].

Jordan, M. I. and Mitchell, T. M. (2015). Machine learning: Trends, perspectives, and prospects. *Science*, 349(6245):255–60.

Julius, D. and Basbaum, A. I. (2001). Molecular mechanisms of nociception. *Nature*, 413(6852):203–10.

Jung, T. P., Makeig, S., Humphries, C., Lee, T. W., McKeown, M. J., Iragui, V., and Sejnowski, T. J. (2000). Removing electroencephalographic artifacts by blind source separation. *Psychophysiology*, 37(2):163–78.

Kandel, E. R. (2013). *Principles of neural science*. McGraw-Hill, New York, 5th edition.

Kennedy, J., Roll, J. M., Schraudner, T., Murphy, S., and McPherson, S. (2014). Prevalence of persistent pain in the u.s. adult population: new data from the 2010 national health interview survey. *J Pain*, 15(10):979–84.

Klimesch, W. (1999). Eeg alpha and theta oscillations reflect cognitive and memory performance: a review and analysis. *Brain Res Brain Res Rev*, 29(2-3):169–95.

Koh, H. K. (2017). Community-based prevention and strategies for the opioid crisis. *JAMA*, 318(11):993–994.

Kragel, P. A., Kano, M., Van Oudenhove, L., Ly, H. G., Dupont, P., Rubio, A., Delon-Martin, C., Bonaz, B. L., Manuck, S. B., Gianaros, P. J., Ceko, M., Reynolds Losin, E. A., Woo, C. W., Nichols, T. E., and Wager, T. D. (2018). Generalizable representations of pain, cognitive control, and negative emotion in medial frontal cortex. *Nat Neurosci*, 21(2):283–289.

Kucyi, A. and Davis, K. D. (2015). The dynamic pain connectome. *Trends Neurosci*, 38(2):86–95.

Kuner, R. and Flor, H. (2017). Structural plasticity and reorganisation in chronic pain. *Nat Rev Neurosci*, 18(2):113.

Kuo, P. C., Chen, Y. T., Chen, Y. S., and Chen, L. F. (2017). Decoding the perception of endogenous pain from resting-state meg. *Neuroimage*.

Kuramoto, Y. (1975). Self-entrainment of a population of coupled non-linear oscillators. In Araki, H., editor, *Mathematical Problems in Theoretical Physics*, volume 39 of *Lecture Notes in Physics, Berlin Springer Verlag*, pages 420–422.

Lachaux, J. P., Rodriguez, E., Martinerie, J., and Varela, F. J. (1999). Measuring phase synchrony in brain signals. *Hum Brain Mapp*, 8(4):194–208.

Latremoliere, A. and Woolf, C. J. (2009). Central sensitization: a generator of pain hypersensitivity by central neural plasticity. *J Pain*, 10(9):895–926.

LeCun, Y., Bengio, Y., and Hinton, G. (2015). Deep learning. *Nature*, 521(7553):436–44.

Lee, U., Kim, M., Lee, K., Kaplan, C. M., Clauw, D. J., Kim, S., Mashour, G. A., and Harris, R. E. (2018). Functional brain network mechanism of hypersensitivity in chronic pain. *Sci Rep*, 8(1):243.

Legrain, V., Iannetti, G. D., Plaghki, L., and Mouraux, A. (2011). The pain matrix reloaded: a salience detection system for the body. *Prog Neurobiol*, 93(1):111–24.

Legrain, V., Perchet, C., and Garcia-Larrea, L. (2009). Involuntary orienting of attention to nociceptive events: neural and behavioral signatures. *J Neurophysiol*, 102(4):2423–34.

Li, L., Wang, H., Ke, X., Liu, X., Yuan, Y., Zhang, D., Xiong, D., and Qiu, Y. (2016). Placebo analgesia changes alpha oscillations induced by tonic muscle pain: Eeg frequency analysis including data during pain evaluation. *Front Comput Neurosci*, 10:45.

Llinas, R., Urbano, F. J., Leznik, E., Ramirez, R. R., and van Marle, H. J. (2005). Rhythmic and dysrhythmic thalamocortical dynamics: Gaba systems and the edge effect. *Trends Neurosci*, 28(6):325–33.

Llinas, R. R., Ribary, U., Jeanmonod, D., Kronberg, E., and Mitra, P. P. (1999). Thalamocortical dysrhythmia: A neurological and neuropsychiatric syndrome characterized by magnetoencephalography. *Proc Natl Acad Sci U S A*, 96(26):15222–7.

Lorente de No, R. (1947). Action potential of the motoneurons of the hypoglossus nucleus. *J Cell Comp Physiol*, 29(3):207–87.

Luck, S. J., Mathalon, D. H., O'Donnell, B. F., Hamalainen, M. S., Spencer, K. M., Javitt, D. C., and Uhlhaas, P. J. (2011). A roadmap for the development and validation of event-related potential biomarkers in schizophrenia research. *Biol Psychiatry*, 70(1):28–34.

Makin, S. (2016). Imaging: Show me where it hurts. *Nature*, 535(7611):S8–9.

Mano, H., Kotecha, G., Leibnitz, K., Matsubara, T., Nakae, A., Shenker, N., Shibata, M., Voon, V., Yoshida, W., Lee, M., Yanagida, T., Kawato, M., Rosa, M. J., and Seymour, B. (2018). Classification and characterisation of brain network changes in chronic back pain: A multicenter study. *Wellcome Open Research*, 3:19.

Mansour, A., Baria, A. T., Tetreault, P., Vachon-Presseau, E., Chang, P. C., Huang, L., Apkarian, A. V., and Baliki, M. N. (2016). Global disruption of degree rank order: a hallmark of chronic pain. *Sci Rep*, 6:34853.

Mansour, A. R., Baliki, M. N., Huang, L., Torbey, S., Herrmann, K. M., Schnitzer, T. J., and Apkarian, A. V. (2013). Brain white matter structural properties predict transition to chronic pain. *Pain*, 154(10):2160–8.

Maris, E. and Oostenveld, R. (2007). Nonparametric statistical testing of eeg- and meg-data. *J Neurosci Methods*, 164(1):177–90.

May, A. (2008). Chronic pain may change the structure of the brain. *Pain*, 137(1):7–15.

May, E. S., Butz, M., Kahlbrock, N., Hoogenboom, N., Brenner, M., and Schnitzler, A. (2012). Pre- and post-stimulus alpha activity shows differential modulation with spatial attention during the processing of pain. *Neuroimage*, 62(3):1965–74.

May, E. S., Nickel, M. M., Ta Dinh, S., Tiemann, L., Heitmann, H., Voth, I., Tölle, T., Gross, J., and Ploner, M. (2018). Prefrontal gamma oscillations reflect ongoing pain intensity in chronic back pain patients. *Hum Brain Mapp*.

Melzack, R. (1987). The short-form mcgill pain questionnaire. *Pain*, 30(2):191–7.

Melzack, R. and Casey, K. (1968). *Sensory, motivational, and central control determinants of pain: a new conceptual model in pain*, pages 423–439. Charles C. Thomas, Springfield, IL.

Meneses, F. M., Queiros, F. C., Montoya, P., Miranda, J. G., Dubois-Mendes, S. M., Sa, K. N., Luz-Santos, C., and Baptista, A. F. (2016). Patients with rheumatoid arthritis and chronic pain display enhanced alpha power density at rest. *Front Hum Neurosci*, 10:395.

Merskey, H. and Bogduk, N. (1994). *Classification of Chronic Pain: Descriptions of Chronic Pain Syndromes and Definitions of Pain Terms*. IASP Press, Seattle.

Moriarty, O., McGuire, B. E., and Finn, D. P. (2011). The effect of pain on cognitive function: a review of clinical and preclinical research. *Prog Neurobiol*, 93(3):385–404.

Mouraux, A. and Iannetti, G. D. (2009). Nociceptive laser-evoked brain potentials do not reflect nociceptive-specific neural activity. *J Neurophysiol*, 101(6):3258–69.

Mouraux, A. and Iannetti, G. D. (2018). The search for pain biomarkers in the human brain. *Brain*.

Mouraux, A., Iannetti, G. D., Colon, E., Nozaradan, S., Legrain, V., and Plaghki, L. (2011). Nociceptive steady-state evoked potentials elicited by rapid periodic thermal stimulation of cutaneous nociceptors. *J Neurosci*, 31(16):6079–87.

Murakami, S. and Okada, Y. (2006). Contributions of principal neocortical neurons to magnetoencephalography and electroencephalography signals. *J Physiol*, 575(Pt 3):925–36.

Nickel, M. M., May, E. S., Tiemann, L., Schmidt, P., Postorino, M., Ta Dinh, S., Gross, J., and Ploner, M. (2017). Brain oscillations differentially encode noxious stimulus intensity and pain intensity. *Neuroimage*, 148:141–147.

Nir, R. R., Sinai, A., Moont, R., Harari, E., and Yarnitsky, D. (2012). Tonic pain and continuous eeg: prediction of subjective pain perception by alpha-1 power during stimulation and at rest. *Clin Neurophysiol*, 123(3):605–12.

Nunez, P. and Srinivasan, R. (2006). *Eletric Fields of the Brain: The Neurophysics of EEG*. Oxford University Press, New York, 2nd edition edition.

Okada, Y. C., Wu, J., and Kyuhou, S. (1997). Genesis of meg signals in a mammalian cns structure. *Electroencephalogr Clin Neurophysiol*, 103(4):474–85.

Oostenveld, R., Fries, P., Maris, E., and Schoffelen, J. M. (2011). Fieldtrip: Open source software for advanced analysis of meg, eeg, and invasive electrophysiological data. *Comput Intell Neurosci*, 2011:156869.

Peirs, C. and Seal, R. P. (2016). Neural circuits for pain: Recent advances and current views. *Science*, 354(6312):578–584.

Peng, W., Hu, L., Zhang, Z., and Hu, Y. (2014). Changes of spontaneous oscillatory activity to tonic heat pain. *PLoS One*, 9(3):e91052.

Pinheiro, E. S., Queiros, F. C., Montoya, P., Santos, C. L., Nascimento, M. A., Ito, C. H., Silva, M., Nunes Santos, D. B., Benevides, S., Miranda, J. G., Sa, K. N., and Baptista, A. F. (2016). Electroencephalographic patterns in chronic pain: A systematic review of the literature. *PLoS One*, 11(2):e0149085.

Plaghki, L. and Mouraux, A. (2005). Eeg and laser stimulation as tools for pain research. *Curr Opin Investig Drugs*, 6(1):58–64.

Ploner, M., Gross, J., Timmermann, L., Pollok, B., and Schnitzler, A. (2006). Pain suppresses spontaneous brain rhythms. *Cereb Cortex*, 16(4):537–40.

Ploner, M. and May, E. S. (2018). Electroencephalography and magnetoencephalography in pain research - current state and future perspectives. *Pain*, 159:206–211.

Ploner, M., Sorg, C., and Gross, J. (2017). Brain rhythms of pain. *Trends Cogn Sci*, 21(2):100–110.

Polania, R., Nitsche, M. A., and Ruff, C. C. (2018). Studying and modifying brain function with non-invasive brain stimulation. *Nat Neurosci*, 21(2):174–187.

Politis, M. (2014). Neuroimaging in parkinson disease: from research setting to clinical practice. *Nat Rev Neurol*, 10(12):708–22.

Rauschecker, J. P., May, E. S., Maudoux, A., and Ploner, M. (2015). Frontostriatal gating of tinnitus and chronic pain. *Trends Cogn Sci*, 19(10):567–78.

Reardon, S. (2015). Neuroscience in court: The painful truth. *Nature*, 518(7540):474–6.

Rice, A. S., Smith, B. H., and Blyth, F. M. (2016). Pain and the global burden of disease. *Pain*, 157(4):791–6.

Rosa, M. J. and Seymour, B. (2014). Decoding the matrix: benefits and limitations of applying machine learning algorithms to pain neuroimaging. *Pain*, 155(5):864–7.

Rubinov, M. and Sporns, O. (2010). Complex network measures of brain connectivity: uses and interpretations. *Neuroimage*, 52(3):1059–69.

Rudd, R. A., Seth, P., David, F., and Scholl, L. (2016). Increases in drug and opioid-involved overdose deaths - united states, 2010-2015. *MMWR Morb Mortal Wkly Rep*, 65(50-51):1445–1452.

Rutkow, L. and Vernick, J. S. (2017). Emergency legal authority and the opioid crisis. *N Engl J Med*, 377(26):2512–2514.

Sarnthein, J. and Jeanmonod, D. (2008). High thalamocortical theta coherence in patients with neurogenic pain. *Neuroimage*, 39(4):1910–7.

Sarnthein, J., Stern, J., Aufenberg, C., Rousson, V., and Jeanmonod, D. (2006). Increased eeg power and slowed dominant frequency in patients with neurogenic pain. *Brain*, 129(Pt 1):55–64.

Schmidt, S., Naranjo, J. R., Brenneisen, C., Gundlach, J., Schultz, C., Kaube, H., Hinterberger, T., and Jeanmonod, D. (2012). Pain ratings, psychological functioning and quantitative eeg in a controlled study of chronic back pain patients. *PLoS One*, 7(3):e31138.

Schmidt-Wilcke, T., Leinisch, E., Ganssbauer, S., Draganski, B., Bogdahn, U., Altmeppen, J., and May, A. (2006). Affective components and intensity of pain correlate with structural differences in gray matter in chronic back pain patients. *Pain*, 125(1-2):89–97.

Schoffelen, J. M. and Gross, J. (2009). Source connectivity analysis with meg and eeg. *Hum Brain Mapp*, 30(6):1857–65.

Scholz, J. and Woolf, C. J. (2002). Can we conquer pain? *Nat Neurosci*, 5 Suppl:1062–7.

Schulz, E., May, E. S., Postorino, M., Tiemann, L., Nickel, M. M., Witkovsky, V., Schmidt, P., Gross, J., and Ploner, M. (2015). Prefrontal gamma oscillations encode tonic pain in humans. *Cereb Cortex*, 25:4407–4414.

Schulz, E., Tiemann, L., Schuster, T., Gross, J., and Ploner, M. (2011). Neurophysiological coding of traits and states in the perception of pain. *Cereb Cortex*, 21:2408–2414.

Seeber, M., Cantonas, L. M., Hoevels, M., Sesia, T., Visser-Vandewalle, V., and Michel, C. M. (2019). Subcortical electrophysiological activity is detectable with high-density eeg source imaging. *Nat Commun*, 10(1):753.

Selim, A. J., Rogers, W., Fleishman, J. A., Qian, S. X., Fincke, B. G., Rothendler, J. A., and Kazis, L. E. (2009). Updated u.s. population standard for the veterans rand 12-item health survey (vr-12). *Qual Life Res*, 18(1):43–52.

Seminowicz, D. A. and Moayedi, M. (2017). The dorsolateral prefrontal cortex in acute and chronic pain. *J Pain*, 18(9):1027–1035.

Seminowicz, D. A., Wideman, T. H., Naso, L., Hatami-Khoroushahi, Z., Fallatah, S., Ware, M. A., Jarzem, P., Bushnell, M. C., Shir, Y., Ouellet, J. A., and Stone, L. S. (2011). Effective treatment of chronic low back pain in humans reverses abnormal brain anatomy and function. *J Neurosci*, 31(20):7540–50.

Seymour, B. (2019). Pain: A precision signal for reinforcement learning and control. *Neuron*, 101(6):1029–1041.

Sherrington, C. (1900). Textbook of physiology, vol. ii, shafer, ea (ed), pentland.

Siegel, M., Donner, T. H., and Engel, A. K. (2012). Spectral fingerprints of large-scale neuronal interactions. *Nat Rev Neurosci*, 13(2):121–34.

Singer, W. (1999). Neuronal synchrony: a versatile code for the definition of relations? *Neuron*, 24(1):49–65, 111–25.

Sitaram, R., Ros, T., Stoeckel, L., Haller, S., Scharnowski, F., Lewis-Peacock, J., Weiskopf, N., Blefari, M. L., Rana, M., Oblak, E., Birbaumer, N., and Sulzer, J. (2017). Closed-loop brain training: the science of neurofeedback. *Nat Rev Neurosci*, 18(2):86–100.

Smith, S. M., Dworkin, R. H., Turk, D. C., Baron, R., Polydefkis, M., Tracey, I., Borsook, D., Edwards, R. R., Harris, R. E., Wager, T. D., Arendt-Nielsen, L., Burke, L. B., Carr, D. B., Chappell, A., Farrar, J. T., Freeman, R., Gilron, I., Goli, V., Haeussler, J., Jensen, T., Katz, N. P., Kent, J., Kopecky, E. A., Lee, D. A., Maixner, W., Markman, J. D., McArthur, J. C., McDermott, M. P., Parvathenani, L., Raja, S. N., Rappaport, B. A., Rice, A. S. C., Rowbotham, M. C., Tobias, J. K., Wasan, A. D., and Witter, J. (2017). The potential role of sensory testing, skin biopsy, and functional brain imaging as biomarkers in chronic pain clinical trials: Immpact considerations. *J Pain*, 18(7):757–777.

Spielberger, C. D., Gorsuch, R. L., Lushene, R., Vagg, P. R., and Jacobs, G. A. (1983). *Manual for the State-Trait Anxiety Inventory*. CA: Consulting Psychologists Press, Palo Alto.

Sporns, O. (2011). The human connectome: a complex network. *Ann N Y Acad Sci*, 1224:109–125.

Sporns, O. (2012). *Discovering the human connectome*. MIT press.

Stam, C. J. (2014). Modern network science of neurological disorders. *Nat Rev Neurosci*, 15(10):683–95.

Stern, J., Jeanmonod, D., and Sarnthein, J. (2006). Persistent eeg overactivation in the cortical pain matrix of neurogenic pain patients. *Neuroimage*, 31(2):721–31.

Tan, L. L., Oswald, M. J., Heinl, C., Retana Romero, O. A., Kaushalya, S. K., Monyer, H., and Kuner, R. (2019). Gamma oscillations in somatosensory cortex recruit prefrontal and descending serotonergic pathways in aversion and nociception. *Nat Commun*, 10(1):983.

The Lancet (2017). The opioid crisis in the usa: a public health emergency. *Lancet*, 390(10107):2016.

Thomson, D. J. (1982). Spectrum estimation and harmonic analysis. *Proceedings of the IEEE*, 70:1055–1096.

Tiemann, L., Hohn, V. D., Ta Dinh, S., May, E. S., Nickel, M. M., Gross, J., and Ploner, M. (2018). Distinct patterns of brain activity mediate perceptual and motor and autonomic responses to noxious stimuli. *Nat Commun*, 9(1):4487.

Tiemann, L., May, E. S., Postorino, M., Schulz, E., Nickel, M. M., Bingel, U., and Ploner, M. (2015). Differential neurophysiological correlates of bottom-up and top-down modulations of pain. *Pain*, 156(2):289–96.

Tracey, I., Woolf, C. J., and Andrews, N. A. (2019). Composite pain biomarker signatures for objective assessment and effective treatment. *Neuron*, 101(5):783–800.

Treede, R. D., Rief, W., Barke, A., Aziz, Q., Bennett, M. I., Benoliel, R., Cohen, M., Evers, S., Finnerup, N. B., First, M. B., Giamberardino, M. A., Kaasa, S., Korwisi, B., Kosek, E., Lavand'homme, P., Nicholas, M., Perrot, S., Scholz, J., Schug, S., Smith, B. H., Svensson, P., Vlaeyen, J. W. S., and Wang, S. J. (2019). Chronic pain as a symptom or a disease: the iasp classification of chronic pain for the international classification of diseases (icd-11). *Pain*, 160(1):19–27.

Uhlhaas, P. J., Roux, F., Rodriguez, E., Rotarska-Jagiela, A., and Singer, W. (2010). Neural synchrony and the development of cortical networks. *Trends Cogn Sci*, 14(2):72–80.

Uhlhaas, P. J. and Singer, W. (2006). Neural synchrony in brain disorders: relevance for cognitive dysfunctions and pathophysiology. *Neuron*, 52(1):155–68.

Upadhyay, J., Geber, C., Hargreaves, R., Birklein, F., and Borsook, D. (2018). A critical evaluation of validity and utility of translational imaging in pain and analgesia: Utilizing functional imaging to enhance the process. *Neurosci Biobehav Rev*, 84:407–423.

Vachon-Presseau, E., Tetreault, P., Petre, B., Huang, L., Berger, S. E., Torbey, S., Baria, A. T., Mansour, A. R., Hashmi, J. A., Griffith, J. W., Comasco, E., Schnitzer, T. J., Baliki, M. N., and Apkarian, A. V. (2016). Corticolimbic anatomical characteristics predetermine risk for chronic pain. *Brain*, 139(Pt 7):1958–70.

van den Broeke, E. N., Wilder-Smith, O. H., van Goor, H., Vissers, K. C., and van Rijn, C. M. (2013). Patients with persistent pain after breast cancer treatment show enhanced alpha activity in spontaneous eeg. *Pain Med*, 14(12):1893–9.

van Diessen, E., Numan, T., van Dellen, E., van der Kooi, A. W., Boersma, M., Hofman, D., van Lutterveld, R., van Dijk, B. W., van Straaten, E. C., Hillebrand, A., and Stam, C. J. (2015). Opportunities and methodological challenges in eeg and meg resting state functional brain network research. *Clin Neurophysiol*, 126(8):1468–81.

van Veen, B. D., van Drongelen, W., Yuchtman, M., and Suzuki, A. (1997). Localization of brain electrical activity via linearly constrained minimum variance spatial filtering. *IEEE Trans Biomed Eng*, 44(9):867–80.

Vanneste, S., Ost, J., Van Havenbergh, T., and De Ridder, D. (2017). Resting state electrical brain activity and connectivity in fibromyalgia. *PLoS One*, 12(6):e0178516.

Vanneste, S., Song, J.-J., and De Ridder, D. (2018). Thalamocortical dysrhythmia detected by machine learning. *Nature Communications*, 9(1).

Velly, A. M. and Mohit, S. (2017). Epidemiology of pain and relation to psychiatric disorders. *Prog Neuropsychopharmacol Biol Psychiatry*.

Vincent, J. L., Patel, G. H., Fox, M. D., Snyder, A. Z., Baker, J. T., Van Essen, D. C., Zempel, J. M., Snyder, L. H., Corbetta, M., and Raichle, M. E. (2007). Intrinsic functional architecture in the anaesthetized monkey brain. *Nature*, 447(7140):83–6.

Vinck, M., Oostenveld, R., van Wingerden, M., Battaglia, F., and Pennartz, C. M. (2011). An improved index of phase-synchronization for electrophysiological data in the presence of volume-conduction, noise and sample-size bias. *Neuroimage*, 55(4):1548–65.

Vingard, E., Mortimer, M., Wiktorin, C., Pernold, R. P. T. G., Fredriksson, K., Nemeth, G., Alfredsson, L., and Musculoskeletal Intervention Center-Norrtalje Study, G. (2002). Seeking care for low back pain in the general population: a two-year follow-up study: results from the music-norrtalje study. *Spine (Phila Pa 1976)*, 27(19):2159–65.

Volkow, N. D. and Collins, F. S. (2017). The role of science in addressing the opioid crisis. *N Engl J Med*, 377(4):391–394.

Vuckovic, A., Hasan, M. A., Fraser, M., Conway, B. A., Nasseroleslami, B., and Allan, D. B. (2014). Dynamic oscillatory signatures of central neuropathic pain in spinal cord injury. *J Pain*, 15(6):645–55.

Wager, T. D., Atlas, L. Y., Lindquist, M. A., Roy, M., Woo, C. W., and Kross, E. (2013). An fmri-based neurologic signature of physical pain. *N Engl J Med*, 368(15):1388–97.

Walton, K. D., Dubois, M., and Llinas, R. R. (2010). Abnormal thalamocortical activity in patients with complex regional pain syndrome (crps) type i. *Pain*, 150(1):41–51.

Wang, X. J. (2010). Neurophysiological and computational principles of cortical rhythms in cognition. *Physiol Rev*, 90(3):1195–268.

Wang, Z., Chen, L. M., Negyessy, L., Friedman, R. M., Mishra, A., Gore, J. C., and Roe, A. W. (2013). The relationship of anatomical and functional connectivity to resting-state connectivity in primate somatosensory cortex. *Neuron*, 78(6):1116–26.

Watts, D. J. and Strogatz, S. H. (1998). Collective dynamics of 'small-world' networks. *Nature*, 393(6684):440–2.

Womelsdorf, T., Valiante, T. A., Sahin, N. T., Miller, K. J., and Tiesinga, P. (2014). Dynamic circuit motifs underlying rhythmic gain control, gating and integration. *Nat Neurosci*, 17(8):1031–9.

Woo, C. W., Chang, L. J., Lindquist, M. A., and Wager, T. D. (2017a). Building better biomarkers: brain models in translational neuroimaging. *Nat Neurosci*, 20(3):365–377.

Woo, C. W., Schmidt, L., Krishnan, A., Jepma, M., Roy, M., Lindquist, M. A., Atlas, L. Y., and Wager, T. D. (2017b). Quantifying cerebral contributions to pain beyond nociception. *Nat Commun*, 8:14211.

Zhang, Z., Gadotti, V. M., Chen, L., Souza, I. A., Stemkowski, P. L., and Zamponi, G. W. (2015). Role of prelimbic gabaergic circuits in sensory and emotional aspects of neuropathic pain. *Cell Rep*, 12(5):752–9.

Zhang, Z., Hu, L., Hung, Y., Mouraux, A., and Iannetti, G. (2012). Gamma-band oscillations in the primary somatosensory cortex - a direct and obligatory correlate of subjective pain intensity. *J Neurosci*, 32:7429–7438.